EVALUATING APOENZYME-COENZYME-SUBSTRATE INTERACTIONS OF METHANE MONOOXYGENASE WITH AN ENGINEERED ACTIVE SITE FOR ELECTRON-HARVESTING: A COMPUTATIONAL STUDY

A Thesis

by

SIKAI ZHANG

Submitted to the Office of Graduate and Professional Studies of
Texas A&M University
in partial fulfillment of the requirements for the degree of

MASTER OF SCIENCE

Chair of Committee,	Sandun Fernando
Co-Chair of Committee,	R. Karthikeyan
Committee Member,	Carmen Gomes
Head of Department,	Steve Searcy

December 2017

Major Subject: Biological and Agricultural Engineering

ABSTRACT

Energy generation via natural gas is viewed as one of the most promising environmentally friendly solutions for ever-increasing energy demand. Of the several alternatives available, natural gas-powered fuel cells are considered to be one of the most efficient for producing energy.

Biocatalysts, present in methanotrophs, known as methane monooxygenases (MMOs) are well known for their ability to quite effectively activate and oxidize methane at low-temperature. To utilize MMOs effectively in a fuel cell, the enzymes should be directly attached onto the anode. However, there is a knowledge gap on how to attach MMOs to an electrode and once attached the impact of active site modification on enzyme functionality.

The overall goal of this work was to computationally evaluate the feasibility of attaching MMOs to a metal electrode and evaluate its functionality using docking and molecular dynamic (MD) simulations. It is surmised that MMOs could be attached to a metal electrode by engineering the active site, i.e., Flavin Adenine Dinucleotide (FAD) coenzyme to attract metal clusters (surfaces) via Fe-S functionalization and such modification will keep the active site functionality unfettered. This work was geared toward performing a structural analysis to identify the spatial distribution of FAD binding site(s) in correlation to Nicotinamide Adenine Dinucleotide (NAD) and subsequently to evaluate the feasibility of utilizing FeS-functionalized FAD for anchoring the enzyme system to a metal electrode.

This work is intended to provide valuable mechanistic insights on critical chemical

reactions that occur within the apoenzyme/coenzyme system and electron transport pathways so that future researchers could utilize the knowledge when fabricating MMO- based electrodes to be used in fuel cells.

DEDICATION

This work is dedicated to my family who are always with me and supporting me from overseas and those who are still under intensive lab work guided by their aspiration of the truth.

ACKNOWLEDGEMENTS

I would like to thank my committee chair, Dr. Fernando, and my co-chair, Dr. Karthikeyan, and committee member Dr. Gomes for their inspiration and advice that guided me throughout the course of this research. Also thanks to my colleagues, friends and other departmental faculty and staff members who offered me suggestions and happiness during stressful work.

CONTRIBUTORS AND FUNDING SOURCES

Contributors

This work was supervised by a thesis committee consisting of Professor Sandun Fernando, R. Karthikeyan, and Carmen Gomes of the Department of Biological and Agricultural Engineering.

The data analyzed for Section 2 was provided by Professor Sandun Fernando. The revision and editorial refinement were conducted in part by Professor R. Karthikeyan. All other work conducted for the thesis was completed by the student independently.

Funding Sources

There are no outside funding source to acknowledge related to the research and compilation of this document.

TABLE OF CONTENTS

Page

LIST OF FIGURES

I. INTRODUCTION AND LITERATURE REVIEW

Methane is an industrially significant raw material that could be produced from petroleum as well as biological sources. Despite abundance, usage of methane as an industrial chemical has been hindered due to its high thermodynamic stability requiring high temperatures for chemical activation – especially when using inorganic catalysts. It has been reported that temperatures as high as 650oC are required for direct-methane fuel cells using ceria-based anodes (Murray, Tsai et al. 1999) whereas the working temperatures for platinum-based catalysts have been still as high as 215oC (Zimmermann, Soorholtz et al. 2016). Nevertheless, methane monooxygenase (MMO) based enzymatic catalysts are known to achieve methane activation at considerably lower temperatures (20 ~37℃) (Fersht 1999, Sirajuddin, Barupala et al. 2014). The motive for using biocatalysts for industrial activation of methane stems from relatively low temperatures required breaking the highly stable C-H bond(s).

Gaining insights from how MMO enzyme system achieves methane activation with such lower energy penalty may provide valuable insights on how to activate methane under abiotic conditions. Many advances have been made since the last review on biological activation of methane (Hanson and Hanson 1996, Culpepper and Rosenzweig 2012), and in this work, we attempt compiling recent advances in the field paying particular attention to mechanistic and functional aspects of enzymatic catalysis of methane.

II. STRUCTURE, FUNCTION AND MOLECULAR INTERACTIONS OF SOLUBLE AND PARTICULATE METHANE MONOOXYGENASES[1]

2.1 Methanotrophic Bacteria

Methanotrophic bacteria, also known as methanotrophs, are a subset of aerobic organ- isms that are capable of metabolizing methane (CH_4) as their only source of carbon and energy (Bakan, Nevins et al. 2013, Lee, McCormick et al. 2013). They can grow aerobically or anoxic (Hyder, Meyers et al. 1979) and survive on the one carbon compound, CH_4. Methane, a naturally occurring organic compound found in abundance as a primary component in natural gas, is thermodynamically very stable. Biological methane metabolism is industrially relevant mainly because biocatalysts are capable of oxidizing me- thane at room temperature while high energy penalty for breaking the first C-H bond(s) exists. (Murray, Tsai et al. 1999) If the thesis is written using the *section method*, the major heading will consist of a title, centered and in all capital letters. This heading may be numbered (Arabic or Roman) or unnumbered. If you are numbering your subheadings by section (1.1, 1.2, etc.), you must number your major headings. Do not use the word “chapter” in your text since your work is not organized in chapters. No punctuation occurs at the end of section titles.

---

[1] Reprinted with permission from"Low-temperature biological activation of methane: Structure, function and molecular interactions of soluble and particulate methane monooxygenases" by Sandun Fernando, Ph.D.; Raghupathy Karthikeyan; Sikai Zhang, 2017. Reviews in Environmental Science and BioTechnology, Volume 16, Page Range 611-623, Copyright [2017] by RightsLink / Springer.

2.1.1 Taxonomy and Physiology of Methanotrophic Bacteria

The first methanotrophs were isolated in 1906; however, only later in 1970, Whittenbury and his colleagues characterized over 100 new methane-utilizing bacteria establishing the basis of current classification of these bacteria (Jiang, Chen et al. 2010). According to the current methodology, methanotrophs are classified as Type I, including the genera Methylomonas and Methylobacter, Methylococcus and Type II, including the genera Methylosinus and Methylocystis primarily based on the two CH4 metabolizing pathways (Fig. 1) (Hanson and Hanson 1996).

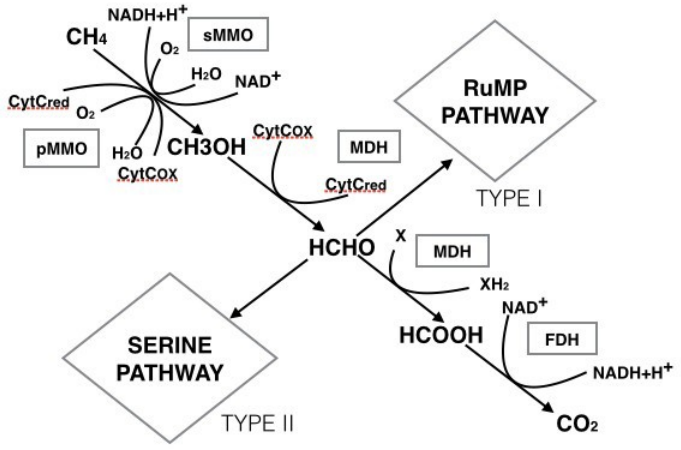

Figure 1 Primary pathways of methane metabolism in methanotrophs.

Type I organisms use Ribulose Monophosphate Pathway (RuMP) whereas Type II uses serine pathway. Recent literature also identifies a Type x that uses a hybridized pathway similar to that of Type I but also utilizes low levels of serine pathway enzymes (Hanson and Hanson 1996). Primary characteristics of Type I and II methanotrophs are shown in Table 1(Hanson and Hanson 1996).

Table 1: Morphological and biochemical characteristics of Type I and II methanotrophs.

Characteristic	Type I	Type II
Cell morphology	Short rods, usually over singly, some cocci or ellipsoids	Crescent-shaped rods, rods, pear-shape sometimes occur rosettes
Growth at 45℃	×	×
G+C content of DNA (mol%)	49-60	62-67
Bundles of vesicular disks	✓	×
Paired membranes aligned to periphery of cells	×	✓
Nitrogen fixation	×	✓
Exospores	×	Few strains
Cysts	Few strains	Few strains
RuMP pathway present	✓	×
Serine pathway present	×	✓
Example Species	*Methylococcus, Methylomicrobium, Methylobacter, Methylomonas*	*Methylosinus, Methylocystis*

One of the main physiological differences of Type I and Type II is that Type I methanotrophs have an internal membrane that is arranged as bundles of vesicular discs while Type II have membranes arranged around the peripheral cell (Hanson and Hanson 1996). More specifically, Type I methanotrophs possess a more uniform membrane structure which is encapsulating cytoplasm homogeneously. Their cytoplasm consists of

a stacked series of flattened discoidal vesicles. Early studies on methanotrophs taxonomy have shown such a uniform morphology of these structures. When subjected to detailed evaluation, extensive internal membrane continuum similar to this exo-membrane occupying most of the cell volume can be observed. However, few researchers have alluded to the fact that instead of being stable, the internal morphology of this type of methane utilizer is critically determined by the environmental growth conditions and the culture age (Hyder, Meyers et al. 1979). On the culture age, they mentioned that those types of microorganisms would have the usual orderly array of the membrane in exponential growth phase and a less diverse and orderly array after they age to stationary phase (De Boer and Hazeu 1972). On the growth conditions, the presence of these membranes has only been observed when the methanotrophs are grown in methanol concentrated environment.

However, organisms are largely filled with electron-lucent droplets, but transfer back to growth on methane induced membrane formation, concomitant with a reduction in the number of electron-lucent droplets (Davies and Whittenbury 1970). It has thus been concluded that methane induces intracytoplasmic membranes, however, as has been observed during the growth of Methylococcus strain NCIB 11083 on methanol, the possibility of induction by ammonia, a methane analog, could not be ruled out (Best and Higgins 1981).

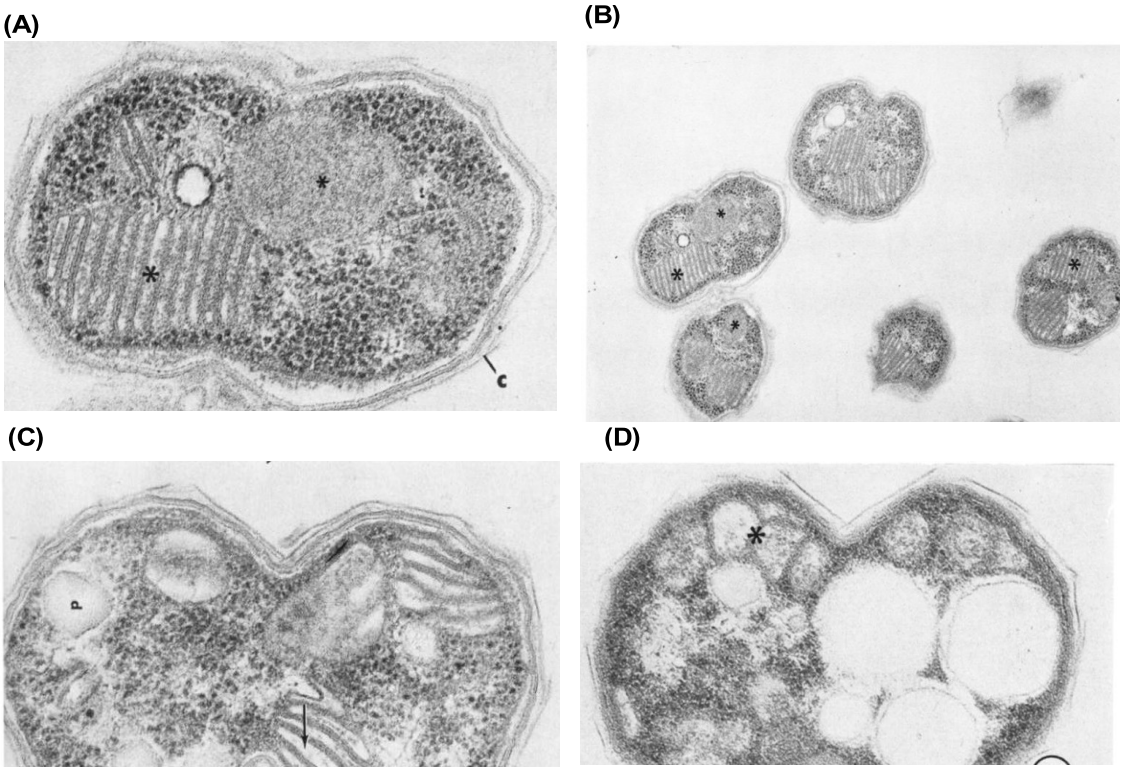

Figure 2: A) Exponential growth phase of Methylococcus spp. when grown on methane. B) Early stationary phase C) late stationary phase D) late stationary phase for Type I (Davies and Whittenbury 1970).

According to Whittenbury and Davis, the intracytoplasmic membranes from Type II methanotrophs grown in methane and methanol are similar (Fig. 2) (Davies and Whitten- bury 1970). Membrane arrays of Type II are less orderly arranged than Type I but more extensive. Membranes of Type II, although are distributed throughout the cytoplasm, in some other sections, are observed to be mainly peripheral. They also reported that the internal arrangement of membranes in organisms of this group, when grown on either me- thane or methanol, was more variable and less ordered than that of the Type I strains (Davies and Whittenbury 1970). The individual membranes, which

were about 80 Å thick and similar to the cytoplasmic membrane in both size and appearance, had the same three-layered structure as the Type I. The membranes were always in pairs and bounded a lumen of varying dimensions which was usually filled with material noticeably less electron-dense than the surrounding cytoplasm (Fig. 2).

2.2 Methane Monooxygenase (MMO)

MMO is an enzyme complex that can oxidize the C-H bonds in methane and other alkanes. As one of the oxidoreductase group, MMO plays a critical role in the first step of methanotrophs metabolism where methane is transformed into methanol (Kao, Chen et al. 2004).

MMO can be divided into two primary types; soluble (sMMO) and particulate (pMMO). Most of the methanotrophs possess both of these types and are expressed in different growth phases based on the concentration of a unique metabolic switch regulated by copper ions. sMMO is expressed while the cell cultures are under low copper conditions (<=0.9 nmol of Cu/mg of cell protein) while pMMO is expressed under relatively high copper/biomass ratios. The structure of sMMO is well understood while information on pMMO is limited (Kao, Chen et al. 2004).

2.2.1 Soluble Methane Monooxygenase (sMMO)

Soluble MMO catalyzes the hydroxylation of methane by dioxygen to methanol via the following reactions:

$NADH = NAD^+ + 2e^- + H^+$

$CH_4 + O_2 + 2H+ + 2e^- = CH_3OH + H_2O$

Overall: $CH_4 + NADH + H^+ + O_2 = CH_3OH + NAD^+ + H_2O$

In this classic monooxygenase reaction, two reducing equivalents from NADH are utilized to split the O-O bond of O2 of which one O atom is reduced to water by 2-electron reduction, while the second is incorporated into the substrate (CH4) to yield methanol (Basch, Mogi et al. 1999). This is the first step in carbon assimilation by methanotrophs. This multicomponent system transfers electrons from NADH through a reductase component to the non-heme di-iron center in the hydroxylase where O2 is activated. Accordingly, the sMMO is composed of three primary subunits that comprise of the hydroxylase, reductase, and the regulatory protein.

2.2.2 Structural Architecture of sMMO

As shown in Fig. 3(Müller, Lugovskoy et al. 2002, Lee, McCormick et al. 2013), sMMO consists of three subunits: a hydroxylase bridged with binuclear iron cluster, an NADH- dependent reductase component containing both flavin adenine dinucleotide (FAD) and ferredoxin [Fe2S2] cofactors, and regulatory protein which controls the reaction between the previous two (Lipscomb 1994).

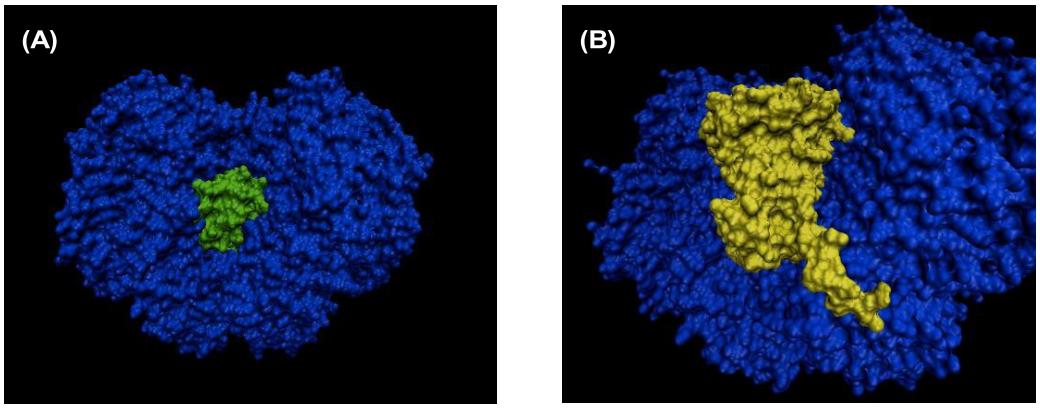

Figure 3: A) sMMO hydroxylase (blue) docked with the regulatory protein (green). B) sMMO hydroxylase docked with reductase (yellow) after the inhibition by regulation.

2.2.3 Methane monooxygenase reductase (MMOR)

Reductase plays a key role in the delivery of electrons within sMMO enzyme systems. MMOR consists of a NAD binding domain, a FAD-binding domain and a ferredoxin (Fig. 4A) (Chatwood 2004). As can be seen both NAD (Fig. 4B) and FAD (Fig. 4C) binding domains reside between residues 1-247. Other reports have assigned residues 0 to 110 for FAD binding domain and 111-251 for NADH binding domain (Chatwood 2004).

The FAD-binding domain consists of one α-helix and a six-stranded antiparallel β-barrel with the first 10 N-terminal residues unstructured (Chatwood 2004). The FAD cofactor is bound in an extended conformation in between two lobes (Fig 4A) (Barik 2004). The NADH-binding domain consists of four α-helices packing closely around a five-stranded parallel β-sheet. As stated by Chatwood, this FAD-reductase is structurally homologous to other FAD-containing oxidoreductases (Chatwood 2004).

Fig. 4 C presents the structure of the Fe2S2 (ferredoxin) domain of sMMO reductase (Müller, Lugovskoy et al. 2002). The protein shown here is a 98-amino acid segment. This structure consists of six β strands arranged into two β sheets as well as three α helices. Two of these helices construct a helix-proline-helix motif, unprecedented among Fe2S2 proteins. The Fe2S2 cluster is a di-iron pair (orange) coordinated by the sulfur atoms (yellow sphere) of cysteine residues 42, 47, 50, and 82. The Fe2S2 domain of the reductase protein transfers electrons to carboxylate-bridged di-iron centers in the hydroxylase component of sMMO. The MMOH binding face of the MMOR Fe2S2 domain was identified using nuclear magnetic resonance (NMR) titration experiment, and according to results, the Fe2S2 cluster appears to be the MMOH (Methane Monooxygenase Hydroxylase) binding site (Müller, Lugovskoy et al. 2002).

Finally, the overall picture of the sMMO reductase reveals an electron pathway as NADH → FAD → [2Fe-2S] → methane monoxygenase hydroxylase (MMOH).

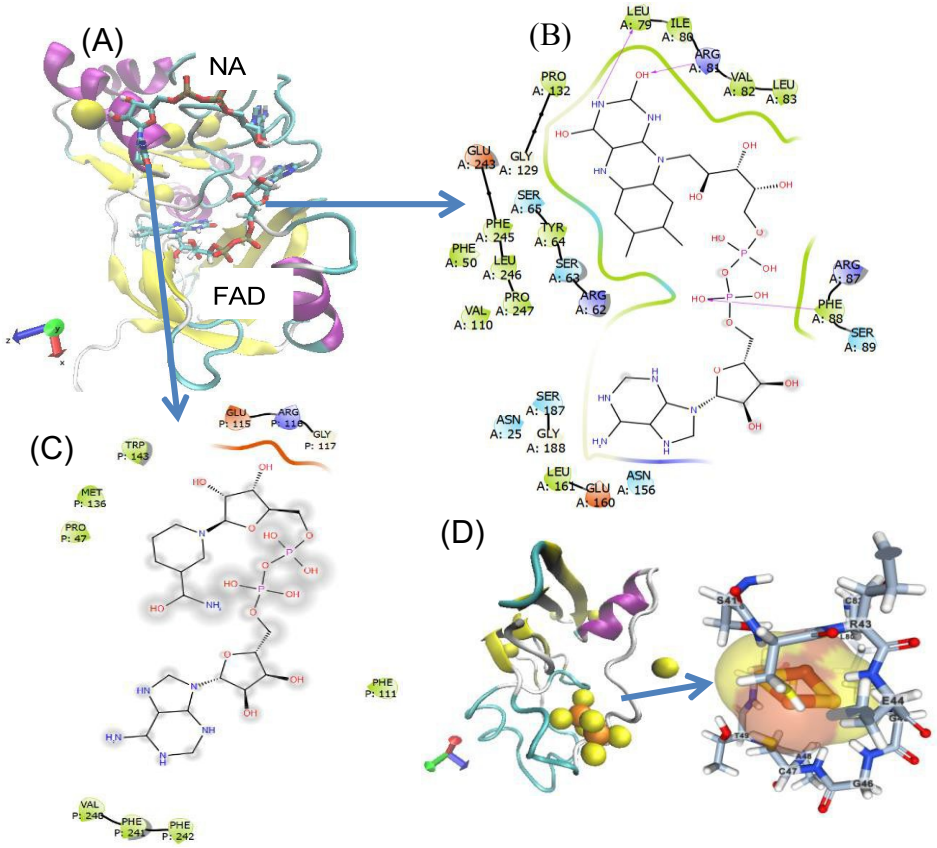

Figure 4: A) Crystal structure of sMMO reductase (1TVC) from Methylococcus capsulatus with NADH/FAD binding domains with FAD ligand; B) Ligand interaction diagram 1TVC with FAD^{+}; C) Ligand interaction diagram 1TVC with NAD^{+}; D) sMMO reductase (1JQ4) Fe_2S_2 (Ferredoxin) site. It should be noted that the FAD interactions presented in Fig. 4 were resolved directly from 1TVC crystal structure whereas NAD interactions were obtained via docking studies since crystallographic data on NAD-bound structures are not available.

2.2.4 Methane Monooxygenase Hydroxylase (MMOH)

The hydroxylase is a flavoprotein that occupies FAD and di-iron center. The hydroxylase consists of three subunits of 60, 45 and 20 kDa arranged in $\alpha_2\beta_2\gamma_2$ configuration (Fig. 5A) and consists almost entirely of the α-helical secondary structure (Lee, McCormick et al. 2013).

Dalton reported a comprehensive structural analysis of MMOH (Dalton 2005). According to him, the subunits are arranged as two αβγ protomers that are related by a non- crystallographic, two-fold symmetry axis. The extensive helical contacts between the α and β subunits of each protomer forms the dimer (Dalton 2005). At the interface between each of the mentioned monomers, a canyon-like area with dimensions of approximately 80 Å×40 Å×20 Å is hence constructed. The γ subunits of MMOH flank the two sides of the hydroxylase and are not involved in dimer formation. The α subunit has the binuclear iron center where methane and oxygen interact to form methanol (Fig. 5B). The interactions of the di-iron center and close residues are depicted in Fig. 5C. The binuclear iron active site resides in a four-helix bundle within the R-subunit, buried beneath the protein surface. Some hydrophobic cavities have been identified by analysis of the MMOH structure, with several in the R-subunit forming a putative pathway from the protein sur- face to the active site (Fig. 5D). The amino acids lining cavities are primarily hydrophobic, suggesting that they may be functionally important for guiding di-oxygen and me- thane to the cavity at the catalytic di-iron center. Other metalloproteins that process gasses for transport or redox functions, such as myoglobin and a Ni-Fe hydrogenase, similarly contain hydrophobic cavities that can accommodate the gaseous substrates (Dalton 2005). The di-iron centers reside in four-helix bundles that are formed by four helices (E through G) in the core of the α subunit as shown in Fig. 5D. Helices E and G each con- tributes a glutamate residue (Glu 114, Glu 209) to the di-iron center, whereas each of the helices H and F donates two iron-coordinating residues in the form of a Glu-Xxx-Xxx-His motif. The remainder of the coordination

sphere is occupied by solvent-derived ligands. Very similar structures occur in other enzymes that use a carboxylate-bridged di- iron center to activate dioxygen, including the R2 subunit of class I ribonucleotide re- ductase and stearoyl-ACP Δ9 desaturase (Dalton 2005).

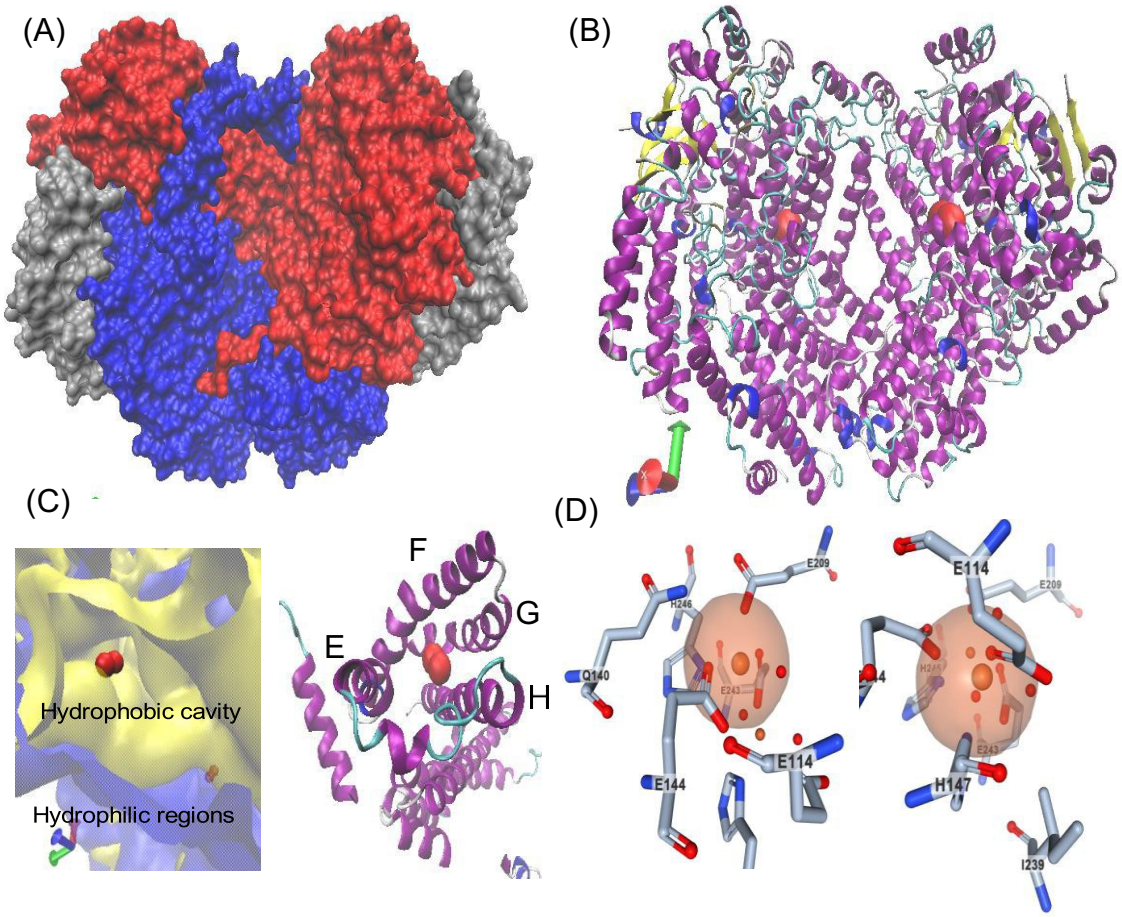

Figure 5: A) Crystal structure of 1XVC with α2 (red) β2 (blue) γ2 (gray) arrangement of sMMO hydroxylase from methylococcus capsulatus; B) sMMO's active sites (red) with secondary structure; C) Beta-helix diagram of four-helix (E – H) bundle; D) Active site interactions with its surrounding residues

2.2.5 Insights from sMMOH docking simulations

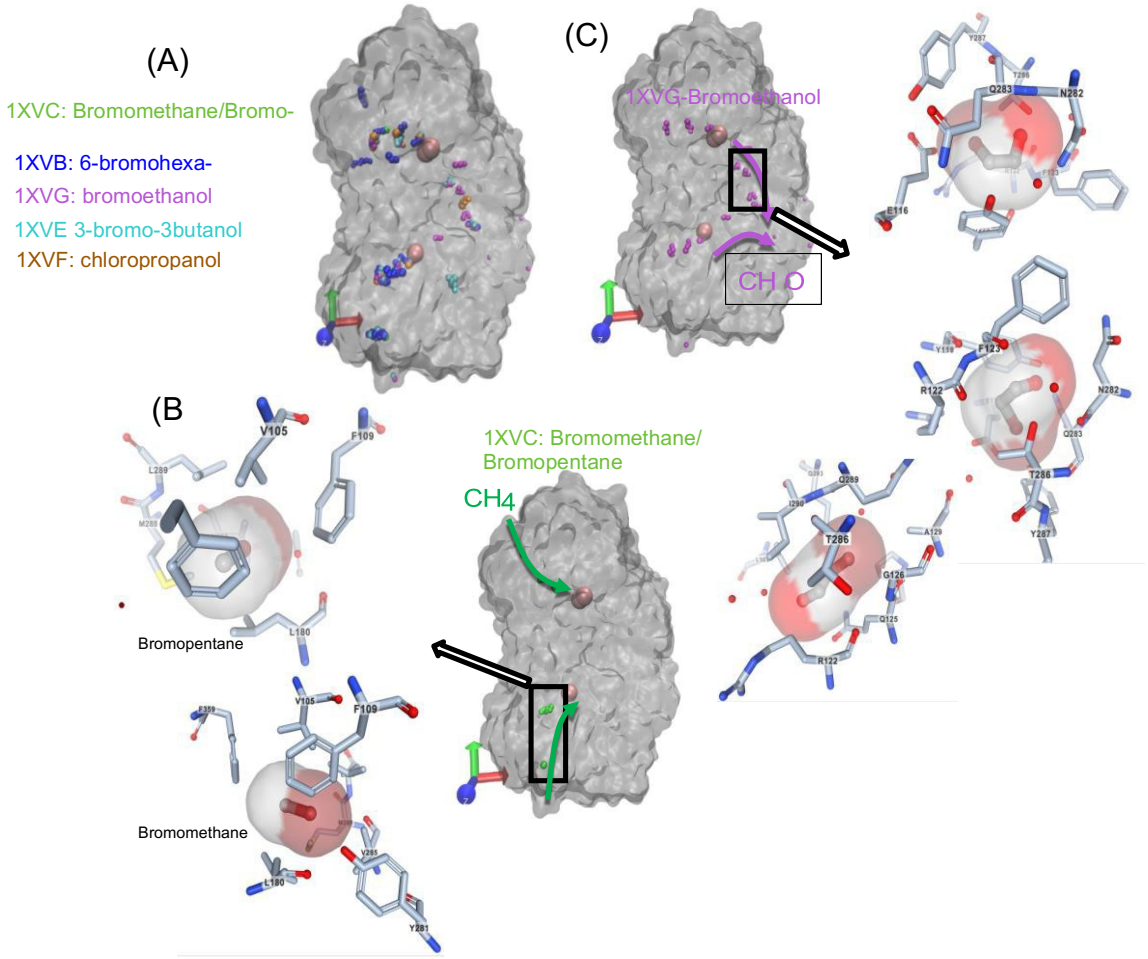

Figure 6 A) Probe distribution on MMOH from methylococcus capsulatus; B) Distribution of bromomethane and bromopentane suggesting the entry path of methane to the di-iron site; C) Bromomethanol distribution suggesting the exit route of theproduct, methanol.

It is reported that the protein that receives and activates methane is the sMMOH (Nordlund 1993). Sazinsky and Lippard indicated that (sMMOH) alpha-subunit contains a series of cavities that define the route of substrate entrance to and product exit from the

carboxylate-bridged di-iron center (Sazinsky and Lippard 2006). They soaked MMOH with a serious of probes to map the possible path and solved the X ray structures of MMOH. The key results are presented in Fig. 6A. By isolating bromomethane and Bromopentaene adhesion sites, it could be surmised the methane entry path is lined with residues V105, F109, L180, Y281, V285, M288 and F35 on chain B followed by L405, L478, L517, V518 and F519 on chain B. As depicted in Fig. 6C the product analogs carve out a path to the surface of the protein hosted by chain C. The probes binding to a position bridging the di-iron sites confirms previous work indicating this site to be where methane is hydroxylated, and methanol is formed.

The sMMOH protein serves not only to supply ligands for the two iron atoms but also to transmit electrons for dioxygen reduction. For a chemical reaction to occur at the di-iron area (active site of sMMOH), electrons, dioxygen, and hydrocarbon substrates all need to be supplied through tightly regulated processes. A sequence alignment analysis of sMMOs, toluene monooxygenases, alkene monooxygenases, and phenol hydroxylases reveals a universally conserved hydrogen-bonding network extending outward from the di-iron site to the hydroxylase surface (Merkx, Kopp et al. 2001). This network included the iron-coordinating histidine residues as well as Tyr 67 and Lys 74 at the protein exterior on helix A in the MMOH canyon and located about 10 Å from the di-iron site (Fig. 6A). A similar hydrogen bonding network is present in the R2 protein of ribonucleotide reductase, where it is proposed to be involved in electron transfer (Merkx, Kopp et al. 2001). It is possible that electron injection into MMOH from MMOR occurs along this pathway.

2.2.6 Regulatory Protein B

Like many other multi-component oxygenase systems, sMMO also has a component of approximately 16 kDa, regulatory protein or B component (Walters, Gassner et al. 1999) (MMOB), which acts as a controller of the methane-to-methanol conversion reaction.

Initial methane oxidation and subsequent hydroxylation occur in the di-iron active center after the conformational change of both the hydroxylase and reductase are mediated by the regulatory protein (B component) (Colby and Dalton 1979, Sazinsky and Lippard 2006). The NADH and disulfide-di-iron clusters reside in the ferredoxin domain of MMOR while the FAD cofactor is residing in the FAD domain. Those two domains play a key hosting role during the reduction of the di-iron center in MMOH. Here, the final electron donor has NADH formed via NAD+ reduction (Colby and Dalton 1979) and the regulatory protein is believed to use this NADH as a coupling pair to regulate product formation. This step is crucial for providing and controlling substrate access to the active site.

The MMOB in low concentrations, can be regulated by proteolysis at its amino terminals, and hence transfer the MMOH into its oxidized state and then stabilize intermediates. These steps are necessary for the oxygen activation. Therefore, it could be surmised that an adequate amount of MMOB can drastically increase the formation of intermediates and speed up the catalytic reaction between methane and methanol (Colby, Stirling et al. 1977).

2.2.7 Catalytic Mechanism of sMMO

During methane oxidation, first, the regulatory protein docks at the α2β2 interface of α2β2γ2 of hydroxylase and therefore triggering a conformational change in the α-subunit. Subsequently, the hydroxylase acts as a proton carrier allowing oxygen and methane interface with the di-iron center. sMMO, according to Lippard's group, would operate just as a NADH rather than a monooxygenase (Lee, McCormick et al. 2013). Another re- port by the same group suggests that ferredoxin domain of the reductase binds to the canyon region of the hydroxylase, which is also where the regulatory protein is bound.

The competitive mechanism between regulatory protein and reductase controls the electron transport (Wang, Iacob et al. 2014). Nordlund and his group performed crystallographic investigations of sMMO hydroxylases. They demonstrated that the structure of sMMO adopted a C2 symmetry with a relatively shallow tunnel on both sides of the protein dimer, which was considered as a potential protein docking site. Afterward, more evidence was provided confirming that this "tunnel" is in fact the position where both the reductase and regulatory proteins are attached on (Colby and Dalton 1979, Stainthorpe, Lees et al. 1990). However, the exact binding site of the reductase component has remained elusive since there is no crystal structure available for the hydroxylase−reductase complex of any MMO enzyme (Wang, Iacob et al. 2014).

By using cross-linking chemical analysis on the sMMO separated from Methylosinus trichosporium OB3b, it has been found that reductase and the regulatory protein are cross- linked to the β-subunit of the hydroxylase MMOH, which implies a competitive mechanism for their binding action. Recently, Lippard et al. managed to explain through hydrogen−deuterium exchange coupled to mass spectrometry (HDX-MS) that the ferredoxin domain of the reductase binds to the "tunnel" region of the hydroxylase, which was determined to be the regulatory protein binding site as well (Wang, Iacob et al.2014). The latter therefore inhibits reductase binding to the hydroxylase and preventing intermolecular electron transfer from the reductase to the hydroxylase di-iron active site.

The specific mechanism of the sMMO system is illustrated in Fig. 7 A (Murrell, Gilbert et al. 2000) and B (Zhang and Lipscomb 2006) and has been proposed by spectroscopic and transient kinetics studies (Zhang and Lipscomb 2006). The resting diferric MMOH is first reduced to diferrous by reduced MMOR. This state reacts with O2 to yield the diferrous intermediate O in which O2 is bound to the enzyme but not to the di-iron cluster. Intermediate O then decays to yield a diferric peroxo or the electronically equivalent mixed-valent superoxo intermediate P*. P* decays to a different diferric peroxo or hydroperoxo species P. Intermediate P then converts to intermediate Q, a unique species that exhibits a relatively intense chromophore at 430 nm. Q has been shown to contain a bis-í-oxo binuclear Fe (IV) cluster that is capable of directly reacting with hydrocarbon substrates to yield the product-bound diferric

intermediate T. The resting diferric state MMOH is regenerated after the release of the product in the rate-limiting step of the catalytic cycle.

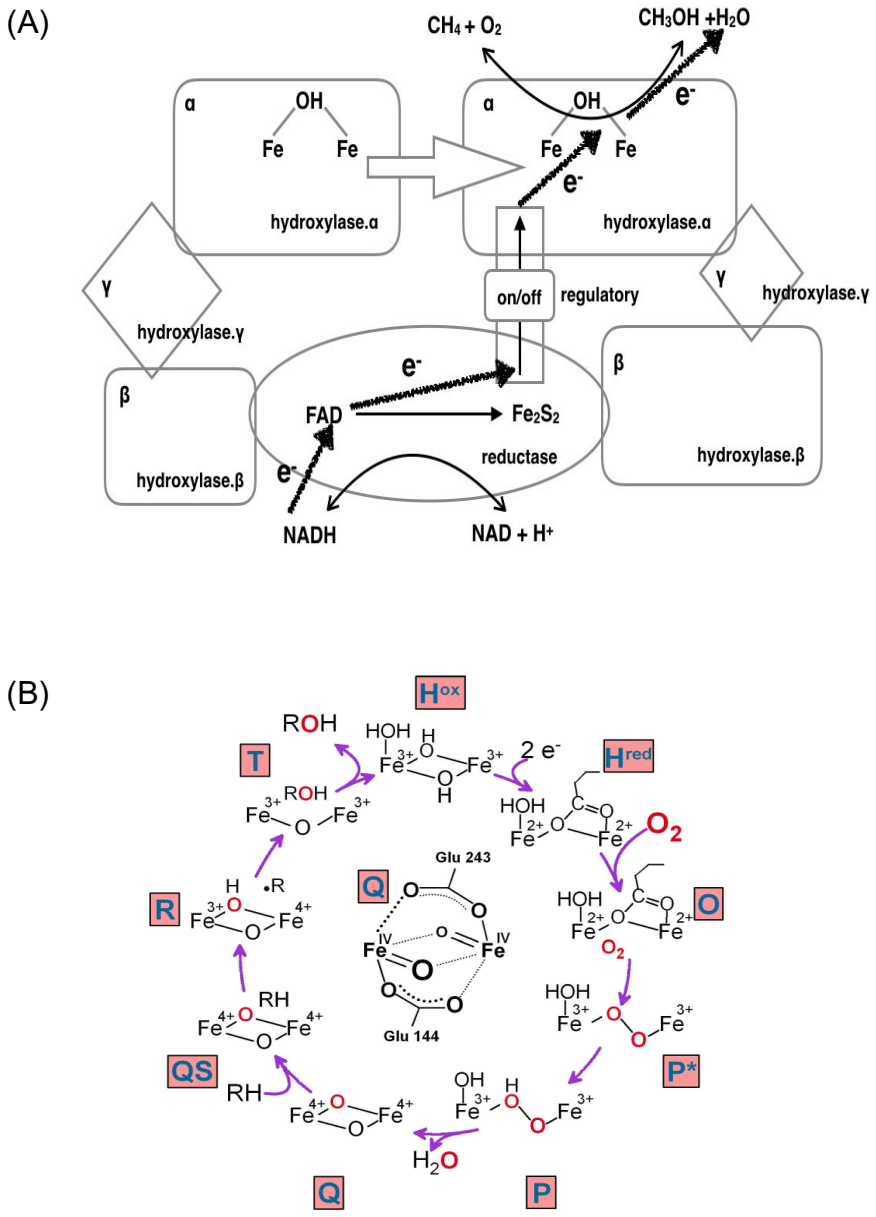

Figure 7: A) Electron transport path and B) reaction mechanism of soluble methane monooxgygenase (Zhang and Lipscomb 2006).

2.2.8 Particulate Methane Monooxygenase (pMMO)

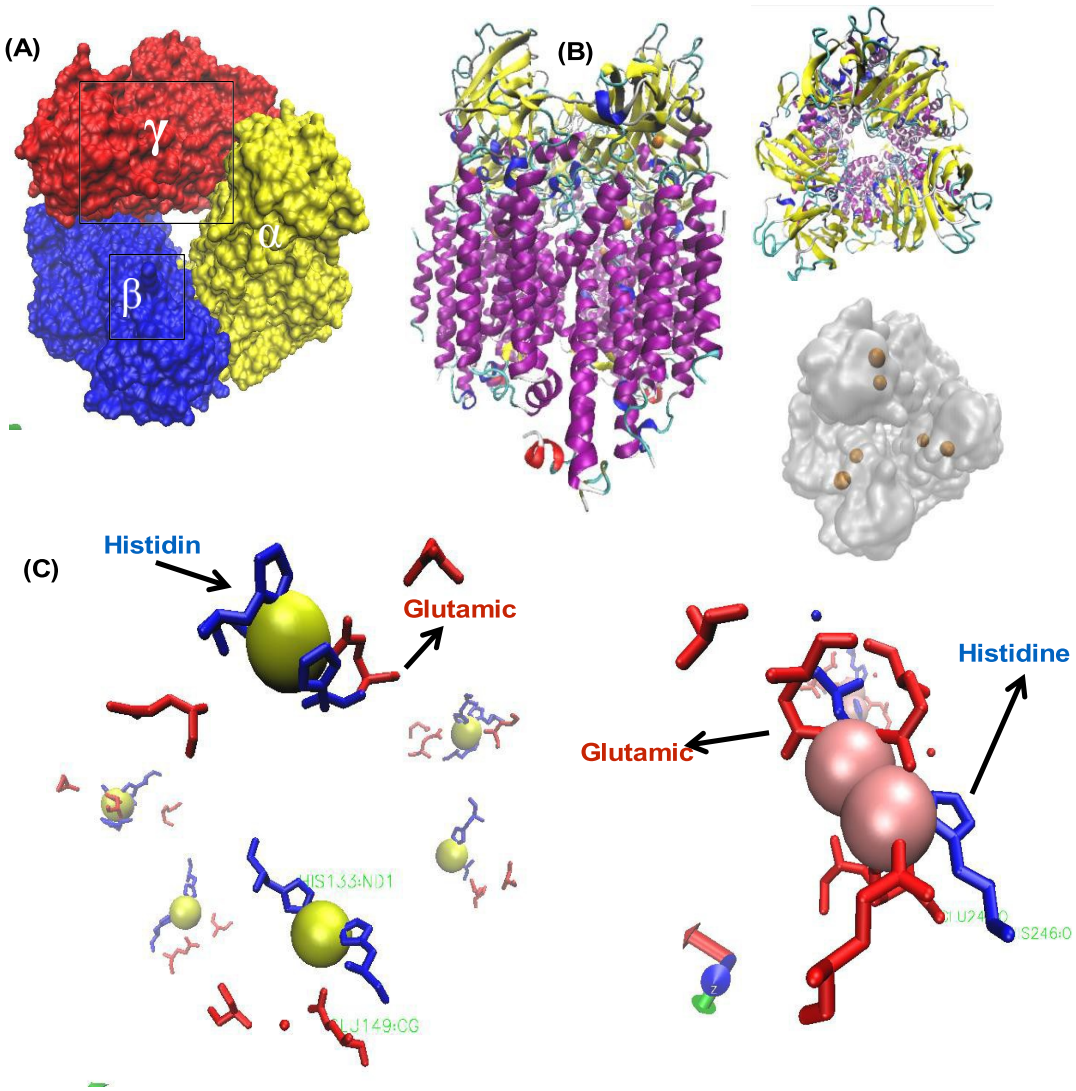

Figure 8: A) crystal structure of pMMO (4PHZ) from *Methylococcus capsulatus*. B) crystal structure of pMMO from *Methylococcus capsulatus* with tri-copper active center; C) interactions of histidine and glutamic acid with the metal centers.

Particulate methane monooxygenase (pMMO) is a membrane-bound metalloenzyme found in methanotrophic bacteria that oxidizes methane into methanol (Sirajuddin and Rosenzweig 2015). Compared to sMMO, the understanding on pMMO is limited due to difficulties in isolating and characterization of the enzyme. However, the crystal structure of pMMO has been solved between 2.8 and 3.9 Å resolutions and deposited as 4PHZ from protein data bank. pMMO possesses a $\alpha_3\beta_3\gamma_3$ trimer composed of the pmoB, pmoA, and pmoC polypeptides and multiple metal binding sites as shown in Fig. 8A (Gassner and Lippard 1999). The metal center consists of multiple copper centers with three hosted by each of the αβγ subsets, where each of pmoA, pmoB, pmoC houses a dicopper center based on the X-ray analysis and a mono-copper center as shown in Fig. 8B. It is also proposed that pMMO active site could possess a di-iron center located at the transmembrane zinc/copper site (Culpepper and Rosenzweig 2012). A model comparison of the soluble and particulate forms of MMO from Methycapsulatus along with MMO from Methylosinus trichosporium OB3b reveals that a commonality exists on interactions of histidine and glutamic acid with the metal centers (Fig. 8C).

2.2.9 Insights from pMMO docking simulations

Although it is well established that methane activation is NAD-dependent, we still do not have any insights on binding locations of NAD on pMMO. To ascertain this, a docking analysis was done with Autodock Vina isolating chains A-D of 4PHZ. The simulations were able to capture cofactor interactions with the exterior surface, as well

as the annular region of the protein. Fig. 9 depicts the most stable binding confirmations of NAD. One NAD molecule docked at the vicinity of SER 33, HIS 133, GLY 130 and PHE 55 while forming an H-bond with SER 33 and close interaction with Cu (301) on the exterior surface of pMMO. The other NAD docked at the vicinity of the second Cu atom lying closer to the annular region of the pMMO while forming close interactions with MET 47, HIS 133 and SER 197 while forming H-bonding with GLY 143 and GLU w149. The availability of NAD binding sites at proximity to Cu atoms confirms the NAD- dependency of methane activation in pMMO similar to sMMO.

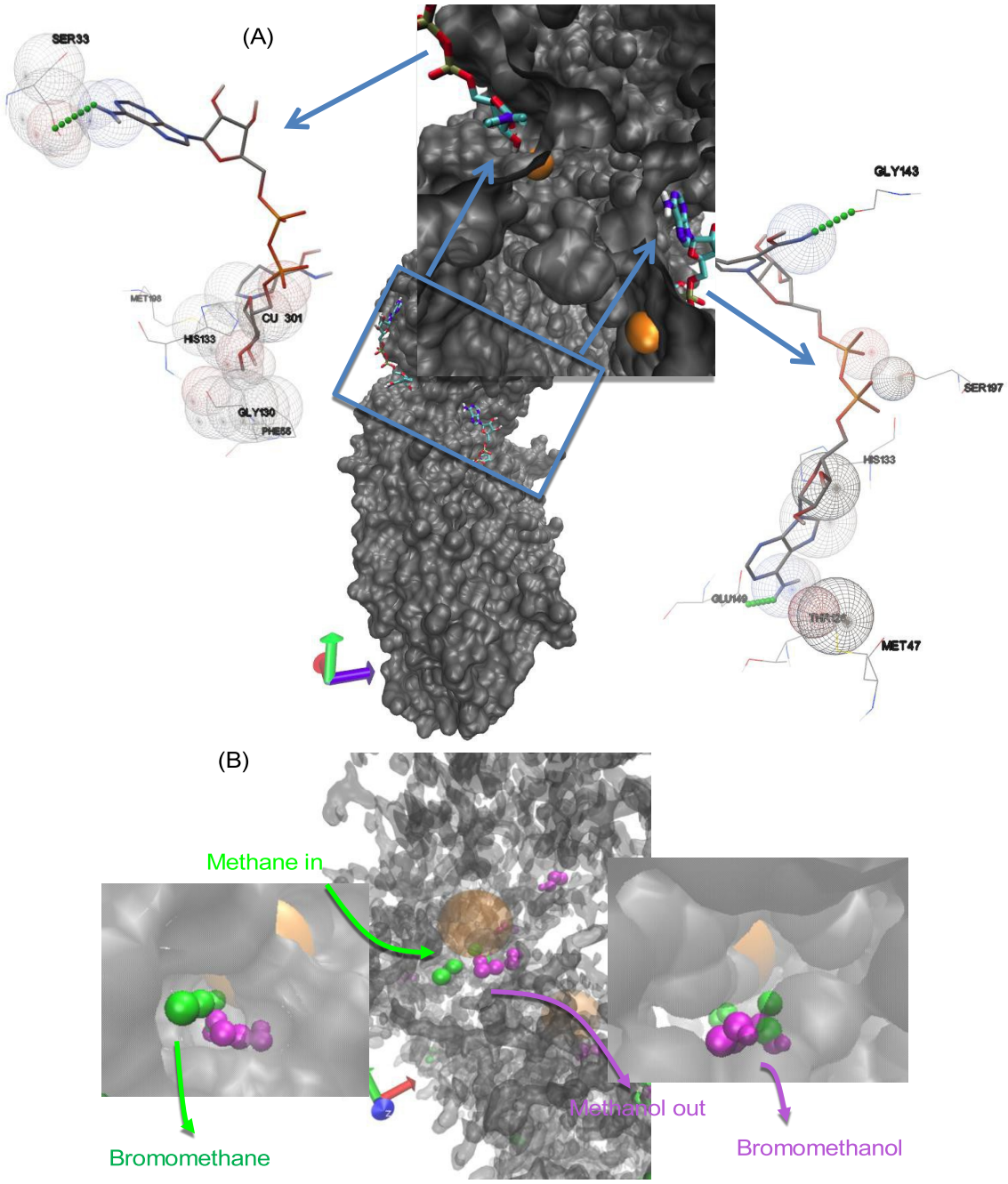

Figure 9: A) NAD docking confirmations with chains A-D of 4PHZ depicting close interactions with Cu centers; B). The path of methane entry and methanol exit deciphers via simulations with bromomethane and bromomethanol.

To get insights on the substrate travel paths to the active site and product exit from the active sites, a docking analysis was done with bromomethane and bromomethanol using Autodock Vina. The two brominated substrates were used to emulate brominated probe analysis done with sMMO (1XVC from protein data bank). The analysis suggests a compelling pathway of methane introduction to the Cu active site that is hosted by residues TRP 35, PRO 80 (A), LEU 84 (A), ILE 91 (A), GLU 93, PRO 107 (A), ARG 108 (A), ALA 109, HIS 123 (A), GLU 167 (A), and PRO 245 (A). The exit canyon is hosted by residues VAL 771 (C) LEU 686 (E), ILE 772 (C), and TYR 516 (B).

2.3 Conclusions

This analysis suggests that in sMMO, low-temperature activation of methane is primarily achieved via Fe-Fe complex in the hydroxylase subunit. The Fe_2S_2 complex in sMMO reductase only acts as a wired mediator to assist electron transport from the NAD/FAD redox couple to the di-iron complex in the hydroxylase. NAD and FAD simultaneously bind to a canyon region located midway between the two lobes in the reductase, forming a continuous wire, assisting the electron transport. The regulatory protein plays a vital role in helping the hydroxylase and reductase subunits to interface and causing conformational changes that control methane oxidation. Methane activation in pMMO occurs at the Cu centers in pMMO. Although the roles of NAD and FAD are well established for sMMO via crystallographic coupled computational analysis, it is not the case for pMMO. However, docking simulations of NAD on pMMO clearly shows preferential binding of the cofactor in the vicinity of the Cu metal centers confirming its

functional relationship with pMMO. Molecular simulations also paint a clear picture of methane travel path from surfaces of sMMO hydroxylase and pMMO to the metal center(s) and exit path of methanol back to the protein surface via a complex set of canyons and tunnels. The analysis suggests sMMO to be the most viable candidate for utilizing MMO in a fuel cell environment due to clearly defined electron transport pathways that are externally accessible and the less likelihood of disrupting methane transport pathways.

III. EVALUATING APOENZYME-COENZYME-SUBSTRATE INTERACTIONS OF METHANE MONOOXYGENASE WITH AN ENGINEERED ACTIVE SITE FOR ELECTRON-HARVESTING: A COMPUTATIONAL STUDY

3.1 Literature Review and Problem Introduction

Low-temperature methane oxidation is one of the greatest challenges in energy research. Although methane monooxygenase (MMO) does this catalysis naturally, how to use this biocatalyst in a fuel cell environment has not yet been investigated. A key requirement to use this enzyme in a fuel cell is wiring of the active site of the enzyme directly to the sup- porting electrode. In soluble MMO (sMMO), two cofactors, i.e., nicotinamide adenine di- nucleotide (NAD^+) and flavin adenine dinucleotide (FAD) provide opportunities for direct attachment of the enzyme system to a supporting electrode. However, once modified to be compatible with a supporting metal electrode via FeS functionalization, how the two cofactors respond to complex binding phenomena is not yet understood. Using docking and molecular dynamic simulations, this study looked at how modified cofactors would interact with sMMO-reductase (sMMOR). Studies revealed that FAD modification with FeS did not interfere with binding phenomena. In fact, FeS introduction significantly improved the binding affinity of FAD and NAD^+ on sMMOR. The simulations revealed a clear thermodynamically more favorable electron transport path for the enzyme system to be used as a fuel cell using FeS-modified-FAD as the anchoring molecule as opposed to using NAD^+. The

overall analysis suggests the strong possibility of building a fuel cell that could catalyze methane oxidation using sMMO as the anode biocatalyst.

Energy generation via natural gas is currently viewed as one of the most promising environmentally friendly solutions for ever-increasing energy demand. Of the several alternatives to producing energy, usage of natural gas in fuel cells seem to be the most efficient (Baldwin, Baase et al. 1998). In this regard, usage of methane as a fuel in high-temperature fuel cells is proven and well established. However, high-temperature fuel cells are limited to stationary applications. If methane is ever to be used for mobile applications, technology should be developed to utilize methane in a low-temperature environment.

Unfortunately, due to the high thermodynamic stability, activation of methane, the primary constituent in natural gas, at low temperature is technically quite challenging. Although inorganic catalysts have been attempted for low-temperature activation (Murray, Tsai et al. 1999), the success has been limited. Nevertheless, biocatalysts, present in methanotrophs, known as methane monooxygenases (MMO) are well known for their ability to quite effectively activate and oxidize methane at low-temperature.

Enzymatic biofuel cells work on the same general principle as all fuel cells; they use a catalyst to separate electrons from a parent molecule and force these electrons to go around an electrolyte barrier through a wire to generate an electric current to power an external load. The enzymatic biofuel cell uses biocatalysts derived from living cells. The enzymes that allow the fuel cell to operate must be "immobilized" (attached) at the

anode (and at times the cathode) for the system to work efficiently; if not immobilized, the enzymes will diffuse into the fuel resulting most of the liberated electrons not reaching the electrodes, compromising its effectiveness.(Whittington, Rosenzweig et al. 2001) The overall effectiveness of all enzyme-based electrochemical devices is dependent on the ability of the molecules that attach enzymes to the electrode to successfully harvest and transport charges from the outer oxidizing point (enzyme active-site) to the inner electrode surface. Accordingly, to utilize MMO effectively in a fuel cell, the enzymes should be directly attached to the anode; however, there is a knowledge gap on how to attach MMO to an electrode and once attached the impact of active site modification on enzyme functionality.

The overall goal of this work was to computationally evaluate the feasibility of attaching MMO to a metal electrode and evaluate its functionality using docking and molecular dynamic (MD) simulations. It is surmised that MMO could be attached to a metal electrode by engineering the active site, i.e., Flavin Adenine Dinucleotide (FAD) coenzyme to at- tract metal clusters (surfaces) via FeS functionalization and such modification will keep the active site functionality unfettered. This work was geared toward performing a structural analysis to identify the spatial distribution of FAD binding site(s) in correlation to NAD+ and subsequently to evaluate the feasibility of utilizing FAD, modified via FeS functionalization, as an anchoring molecule to attach MMO apoenzyme to an electrode via a combination of docking and molecular dynamic simulations. The rationale here is that before attempting fabrication of a fuel cell (anode) in a laboratory, computational studies will provide valuable mechanistic insights on the

approach of "wiring" MMO to the electrode has any practical merit. The approach here is to compare the thermodynamic binding affinities of FeS-modified coenzymes when interacting with MMO apoenzymes so that insights could be made on the strength and stability of such interactions in- silico before attempting fabrication of fuel cell electrodes in the laboratory.

MMO is an enzyme complex found in methanotrophs that can oxidize the C-H bond in methane and other alkanes. Although two primary types of MMO are present, i.e., soluble (sMMO), and particulate (pMMO), for this study sMMO, was chosen due to the availability of extensive structural and functional data as compared to pMMO.

The sMMO is composed of three primary subunits that comprise of a hydroxylase (a hydroxylase-bridged binuclear iron cluster, MMOH), a reductase (a NADH-dependent reductase component containing both FAD and [Fe2S2] cofactors, MMOR) and regulatory protein (Deeth and Dalton 1998). This multicomponent system transfers electrons from NADH through a reductase component to the non-heme diiron center where O2 is activated (Eq. 1) (Chatwood, Müller et al. 2004).

$$CH4 + 2NADPH + O2 = CH3OH + 2NADP+ + 2e + H2O \quad \text{(Eq. 1)}$$

The reductase comprises three distinct domains, a [2Fe-2S] ferredoxin domain along with FAD- and NADH-binding domains (Chatwood, Müller et al. 2004). The hydroxylase is a flavoprotein consisting of three subunits of 60, 45 and 20 kDa arranged in $\alpha 2\beta 2\ \gamma 2$ configuration. The α subunit has the binuclear iron center where methane and oxygen interact to form methanol. Like many other multicomponent oxygenase systems, sMMO also has a component of approximately 16 kDa, regulatory protein, which acts as

a controller of the methane-methanol reaction. Due to the affinity of reductase for coenzymes, reductase was chosen for the interaction studies.

3.2 Approach

3.2.1 Identification of an Anchoring Site and a Ligand

Of the three subunits, reductase and hydroxylase offer the best sites for anchoring the MMO complex to the electrode. A key requirement of the anchoring site is that the ligand should be within the electron transport chain so that the electrons would be harvested to be routed to an external load. Additionally, the ligand docking site should be accessible such that the ligand, once attached to the electrode would still be available for docking. Looking at other enzymatic fuel cells, the best ligands to be tapped for electron harvesting are FAD and NAD^+ coenzymes. There are numerous examples of FAD being modified to be anchored to electrodes in FAD-dependent oxidases (Willner, Heleg-Shabtai et al. 1996, Lin and Chen 2006, Marafon, Kubota et al. 2009) and NAD-dependent hydrogenases (Golabi and Zare 1999, Gorton and Domí 2002, Karyakin, Ivanova et al. 2003) often in the presence of electron mediators.

To this end, the first step was the identification of binding sites and conformations of NAD^+ and FAD on sMMOR. sMMOR was selected as it is reported that the methane oxidation occurs directly on this enzyme and NAD^+ and FAD, the probable candidates as the anchoring ligand(s) are known to interact with sMMOR.

For this evaluation, NMR structure of sMMOR from (Gorton and Domí 2002) Methylo- coccus capsulatus (Bath) (index 1TVC from protein data bank) was used. The NMR struc- ture had the primary NAD^+ binding site(s) already resolved (Chatwood, Müller et al. 2004). However, the FAD-binding sites were not. So, the first step of this analysis was to decipher the FAD-binding site(s).

The approximate vicinity of the binding domain was first resolved via a docking simulation using Autodock and verified by a more in-depth molecular dynamic (MD) simulation using Nanoscale Molecular Dynamics (NAMD).

3.2.2 Autodock Methodology

AutoDock is a suite of C programs used to predict the bound conformations of a small, flexible ligand to a macromolecular target of known structure. The technique combines simulated annealing for conformation searching with a rapid grid-based method of energy evaluation. (Goodsell, Morris et al. 1996).

In this work, AutoDock4 (Goodsell, Morris et al. 1996) was used to predict the conformations of ligand once it is docked on the receptor. For this, initially, the receptor in PDB format was loaded using AutodockTools (ADT) graphical interface. After removal of anyextraneous ligands and ions, polar hydrogens were added, and the file was saved in PDBQT format. The ligand files, when available, were downloaded from chemical databases (E.G., PubChem, ChemSpider, or eMolecules) or created from first principles using Chemisketch chemical modeling (Österberg and Norinder 2001). Once built, the structure was 3D optimized. Different chemical file formats were converted to

PDB format as required by Autodock using OpenBabel. Open Babel is an open-source toolbox that works as a translator between different chemical source formats. (O'Boyle, Banck et al. 2011). In this work, the structure models were initially saved in .MOL2 format which was then converted to .PDB for simulations.

The ligand was prepared in AutoDock by choosing appropriate torsion centers and the number of torsions. In most cases, the default values were used. Then, the ligand file was saved as a PDBQT format. Finally, the search grid was set to cover the entire molecule initially. Once the system was set, the docking conformations were evaluated using the Genetic Algorithm. The simulation output includes a PDBQT file with top ten docking conformations and a log file that contains thermodynamic affinity values for each conformation. The most probable location of coenzyme binding was further verified using NAMD MD simulations.

The target here was to accurately identify the coenzyme binding pocket(s)) in an environment that closely resembles that the protein would encounter in the real world. To achieve this, a simulation system was set up to steer multiple coenzyme molecules to the dynamically changing receptor.

So, to emulate solvent environment, sMMOR was immersed in a water sphere in the presence of the cofactor. The system was minimized and simulated to discern the hotspots where the cofactor would preferentially bind while the protein was still undergoing structural deformation.

3.2.3 Creation of Protein Structure Files and Force-field Parameter Files for sMMOR and Cofactor

To perform MD simulations using NAMD, four distinct files are needed:

- A Protein Data Bank (PDB or.pdb) file (in this case sMMOR) that stores atomic coordinates and/or velocities for the system.
- A Protein Structure File (PSF or .psf) of sMMOR that stores structural information of the protein, such as various types of bonding interactions.
- A force field parameter file that contains the mathematical expressions of the potentials experienced by the atoms in the system. CHARMM, X-PLOR, AMBER, and GROMACS are four types of force fields, and NAMD can use all of them.
The parameter file defines bond strengths, equilibrium lengths, and other variables.
- A configuration file in which the user specifies all the options that NAMD should use in running a simulation. The configuration file tells NAMD how the simulation is to be run.

The PDB file of sMMOR (1TVC) was used as the receptor proteins in the MD simulations, and cofactor was the ligand. The original PDB file of 1TVC was used to build the PSF files. The procedure used to build the PSF files is given elsewhere (O'Boyle, Banck et al. 2011). The PSF file is developed based on the information in the PDB file while taking into consideration any chains that are missing from the original crystal structure. The final PSF file is built after patches are applied. The force field files of the ligands were developed to populate the ligands in the vicinity of the receptor protein and simulate their interactions. CHARMM General Force Fields (CGenFF) were

used for cofactor ligand. The procedure used to develop force field files is given elsewhere (O'Boyle, Banck et al. 2011).

3.2.4 NAMD Simulations With Cofactor Ligands

The ligand binding landscape of sMMOR was initially elucidated by allowing selected ligands to interact with the enzyme via MD simulations. For this initial analysis, a set of small organic molecular probes that consists of selected concentrations of isopropanol, isobutene, acetamide, acetate, and isopropyl amine was used to discern the specific affinity of the protein to these probes (i.e., active species). These small molecules possess the active sites resembling those of the cofactor. Small probes were selected (four non- hydrogen atoms), so they can diffuse rapidly and explore small and even transient pockets via the simulations. This property also helps to sample a large number of binding events, and it enables reaching equilibrium in relatively short simulation times (in this case, approximately one week to several days per simulation). This assessment was performed with the intension of determining any individual "hot spots" or clusters of "hot spots" that indicate the existence of ligandable receptors, their composition, binding affinities, and other electronic and structural features.

Initial system setup: Once the structure (.psf) and coordinate (.pdb) files are available; sMMOR was solvated to more closely resemble the solvent environment. This was done by building a water box which is the preferred configuration due to the elongated shape of the sMMOR. The solvate plugin available in Visual Molecular Dynamics (VMD) was be used for this purpose. Note that a Tcl/Tk programming script

also could be written for this. Any counter ions were added using the auto-ionize plugin. Ligands were added using the drugui plugin. Next, the configuration (.conf) files required to run the NAMD simulation were prepared. Fig. 10 shows the output log file and the solvation box after the system has been set up to run the NAMD simulations for a model protein.

NAMD simulations: NAMD simulations were performed in the High-Performance Computing Center (HPCC) at Texas A&M University. The simulations were performed in the Ada cluster. Ada is an Intel x86-64 Linux cluster with 852 compute nodes (17,340 total cores) and 8 login nodes. Most (792) of the compute nodes are IBM NeXtScale nx360 M4 dual socket servers based on the Intel Xeon 2.5-GHz E5-2670 v2 10-core processor, commonly known as the Ivy Bridge. The other nodes are configured with distinct hardware to enable special functional capabilities (e.g., GPGPU processing; very fast data transfers to external hosts; and login access).
The output files from a NAMD simulation will include velocity trajectory (.vel), coordinate trajectory (.dcd), cell dimensions (.xsc), and log (.log) files.

Probe grid calculation: The coordinate file, structure file, and coordinate trajectory file will be used to calculate the probe grid. The druggui plugin in VMD allows setting up grid resolution (Å); contact distance (Å); hotspot free energy, dG, (kcal/mol); the number of hotspots to the cluster; lowest affinity (mM); and charge (e). Grids were calculated for different types of probes using their central carbon atoms. These grids were merged in the hot-spot analysis described below. A python executable

could be used instead of the plugin. The output files subsequent to the probe grid calculation were .dx files that store occupancy grids of each probe/ligand.

Protein surface analysis for binding hotspots and hotspot clusters: The binding hotspots based on occupancy grids were calculated using the drugui plugin in VMD. This step involves selecting high-affinity probe binding spots, clustering them, and then merging them to assess high-affinity sites. Subsequent to identification of binding landscape with probes, an analogous NAMD simulation was done with the cofactor in place of the probes.

Solvation: Box padding 6 A.

Ionization: System has a total charge of - 9.000009894371033 electrons.
Ionization: 9 sodium ions will be added. Ionization: System is ionized to become neutral.
Statistics: System contains 4880 water and 244 probe molecules
Statistics: System contains 0 isopropanol molecules.
Statistics: System contains 0 isobutane molecules.
Statistics: System contains 244 acetamide molecules.
Statistics: System contains 0 acetate molecules.
Statistics: System contains 0 isopropylamine molecules.
Statistics: System contains 38983 atoms Statistics: Mass of the system is 306926.73669838905 amu
Statistics: Density of the system is 0.6200000000000001 amu/A^3

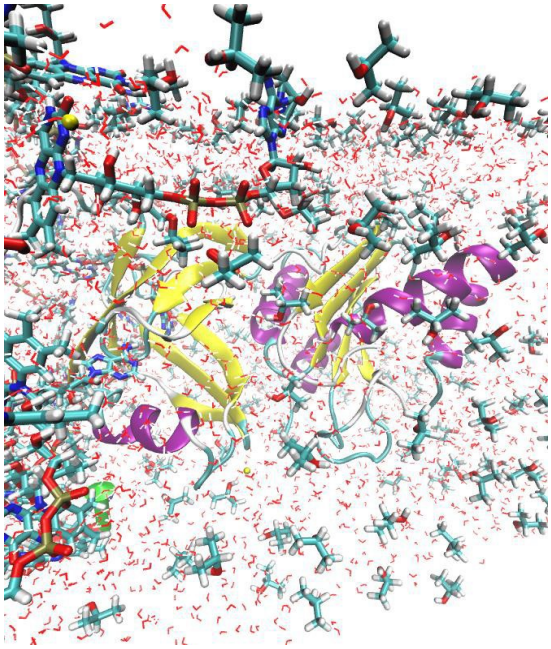

Figure 10: Output log file and solvation box after preparing a model protein system for NAMD simulations.

3.3 Verification Studies

Once the cofactor most suitable for anchoring the apoenzyme to a metal electrode was identified, a series of simulations were done to verify if a modified co-factor, functionalized to attach to a metal electrode would bind onto the active site as anticipated. It should be noted here that based on the results from section 2.1, the FAD was chosen as the ligand of choice for sMMOR anchoring. Accordingly, the methods for

verifying FeS- modified FAD are described hereon. The simulations steps were as follows.

3.3.1 Evaluating Affinity Thermodynamics and Binding Conformations of Modified FAD on sMMOR

The affinity thermodynamics and binding conformations of modified FAD on sMMOR were evaluated using FAD (control), FAD-FeS and FAD-FeS-Ag.

The cofactor molecules were built in Chemsketch software and optimized three dimensionally before being used in simulations. Energy minimization was done using the Molecular Orbital PACkage (MOPAC) program. Whenever needed, molecular formats were changed using the OpenBabel software. Although Au is the standard metal used for enzymatic electrode preparation, Ag clusters had to be used as an alternative metal due to Autodock not being able to support Au simulations. The docking simulations were done in Autodock Vina according to the methods described above.

3.3.2 Evaluating the Impact of Modified FAD Introduction on NAD^+ Binding

For the fuel cell to work as anticipated, it is critical that once FeS-modified FAD is docked, there is adequate clearance for unfettered access of NAD^+ (or vice versa). It is also critical that functionalized FAD and NAD^+ dock such that there is a continuous path for electrons to follow. To evaluate these, NAD^+ docking was simulated on sMMOR already docked with FAD (control) and FAD-FeS-Ag. The docking simulations were done in Autodock Vina according to the methods described above.

3.4 Results and Discussion

3.4.1 Identification of a Ligand Suitable for Anchoring the Enzyme System

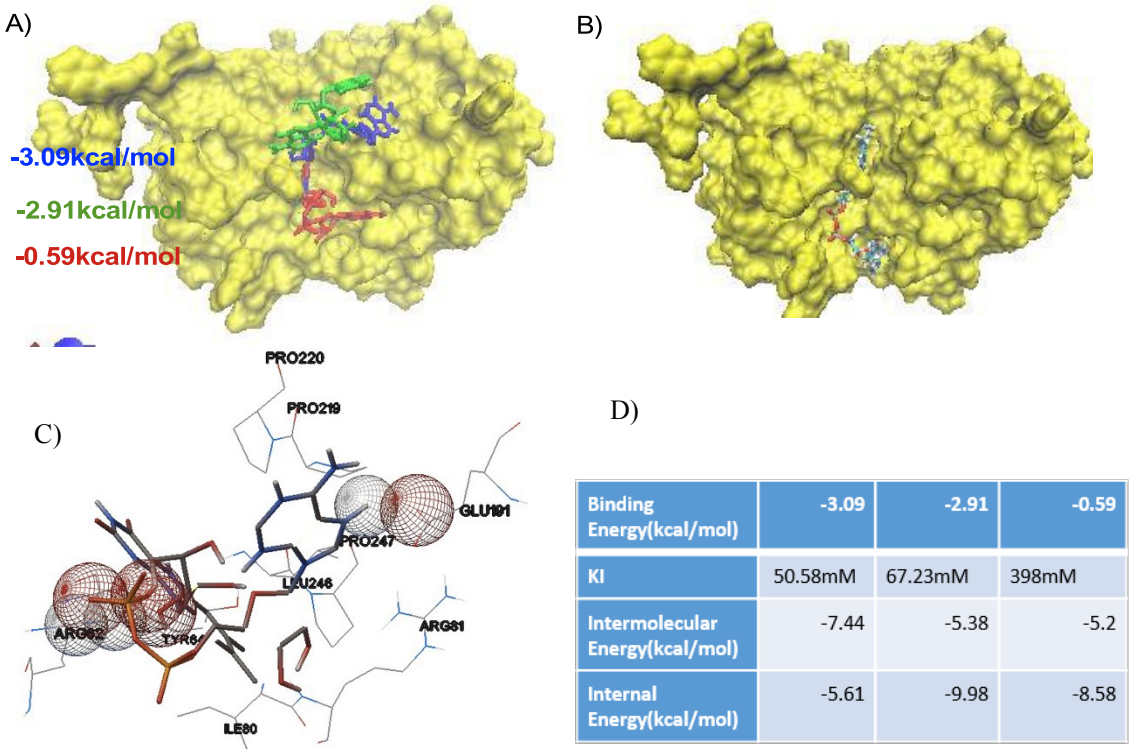

Binding Energy(kcal/mol)	-3.09	-2.91	-0.59
KI	50.58mM	67.23mM	398mM
Intermolecular Energy(kcal/mol)	-7.44	-5.38	-5.2
Internal Energy(kcal/mol)	-5.61	-9.98	-8.58

Figure 11: A) Predicted three most stable conformations of sMMOR (with binding affinity in descending order of blue, green, and red) docked with FAD using AutoDock4; B) Conformations of sMMOR with FAD reported by Lippard's group via experimental verification; C) Interaction diagram of highest possible conformation (blue) of FAD on sMMOR.

Several factors have to be considered when choosing a ligand for anchoring the enzyme system. One key requirement is that the ligand should be an integral part of the electron transport chain. Accordingly, FAD and NAD^+ are key candidates for this. Other factors include the accessibility of the ligand to anchor onto the supporting electrode, the

implications of ligand modification to overall activity and reduction potentials. The docking simulation of FAD and NAD^+ with sMMOR was done to decipher how accessible the ligands would be after binding. The results of the initial docking simulation of sMMOR with FAD is depicted in Figure 11. It could be noted that predictions via Autodock were in close agreement with experimental data (Chatwood, Müller et al. 2004). The simulations predict that the most stable binding conformation of FAD would interact with residues Arginine and Tyrosine of sMMOR via hydrogen bonding. It is evident that FAD binds onto the canyon region that lies on the surface of the protein and thus is accessible to an external (electrode) surface.

The binding conformations and interactions of sMMOR and FAD have been introduced by Lippard and coworkers (Chatwood, Müller et al. 2004). It was disclosed that the sMMOR/FAD-binding domain is highly homologous to several other members of Ferredoxin proteins like benzoate-1,2 dioxygenase reductase from Acinetobacter sp. strain ADP1.

Such a homogeneousness suggests a possible position for the FAD domain on the sMMOR. The FAD-binding domain in sMMOR is composed of an antiparallel Beta barrel with an Alpha-helix at one opening of the barrel. Which is located at the interface of two chains of the protein.

The conformations validated by experimentation by Lippard and coworkers group are shown in Figure 11B (Chatwood, Müller et al. 2004). Lippard et al. reported the bonding interactions between the receptor (sMMO) and ligand (FAD). According to their analysis, adenine group of FAD is held in place by hydrogen bonds involving its

N6 and N7 nitrogen atoms and O3 of the ribityl moiety with or without additional stabilization by stacking of an aromatic residue in the C-terminal region of the protein. The strongest hydrogen bonding came from residue Arg62 and Glu191. This fact is supported by present work which depicts strong hydrogen bonding between H23 of ligand and Arg62 in the receptor (Figure 11B) (Chatwood 2004).

It is evident that the binding energy is relatively low (negative) indicating that the system becomes more stable after sMMOR docked with the FAD. The low intermolecular energy shows a stable environment between the unbounded atoms between the receptor and ligand. Low Internal energy also shows a high stability of the resulting system. Although the inhibitor constant (KI) value is surprisingly high, we consider it still as reasonable as other research had achieved similar values with FAD interacting successfully with its receptor (Yagi and Ozawa 1960).

As the next step, how NAD^+ interacts with sMMOR was elucidated, and the docking results are depicted in Figure 12.

It appears that NAD^+ would have preferred the canyon area similar with FAD's "choice", even with higher affinity. This area provides a stable conformational structure for ligand to be docked.

A)

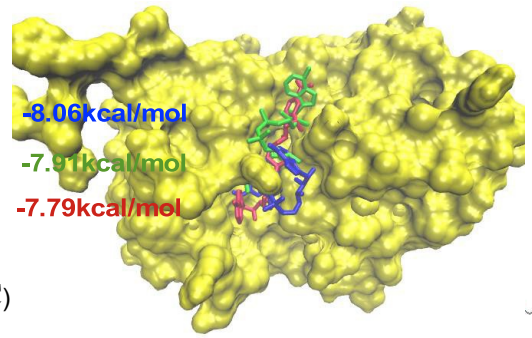

B)

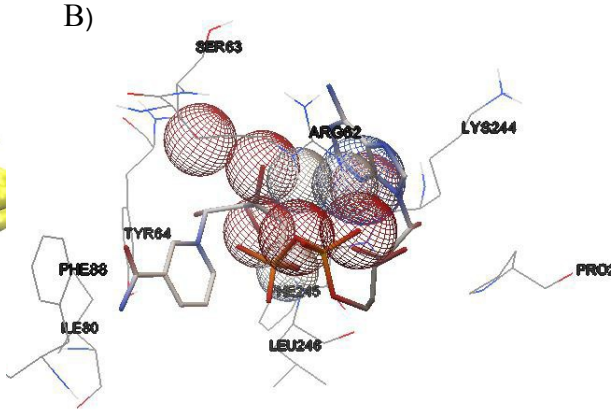

C)

Binding Energy(kcal/mol)	-8.06	-7.91	-7.70
KI(mM)	34mM	38mM	56mM
Intermolecular Energy(kcal/mol)	-12.53	-12.39	-12.27
Internal Energy(kcal/mol)	-0.63	-0.32	-0.68

Figure 12: A) Predicted three most stable conformations of sMMOR (with binding affinity in descending order of blue, green, and red) docked with NAD^+ using AutodDock4. B) Interaction diagram of highest possible conformations of NAD+ on sMMOR; C) Thermodynamic data.

In terms of electron transportation in the natural system (how methanotrophs metabolize methane naturally), it has been reported that sMMO system transfers electrons from NADH through sMMOR to the non-heme di-iron center in where O_2 is activated (Chatwood 2004). The docking simulations show that NAD^+ lies on the right side of FAD domain, within the pocket just above the canyon where the FAD is located confirming experimental results facilitating effective electron transport from cofactors to the di-iron active site. The inter- action diagram (Figure 11 C) shows that the hydrogen bonds are formed between FAD and sMMOR with residues Val 83, Lys244 and Phe242, while residues Phe245, Arg62 form hydrogen bonding with NAD^+. The spatial

distribution of the two cofactors suggested NAD to be located more favorably facilitating binding with an external surface.

A NAMD molecular dynamic simulation was conducted to further clarify the location of FAD binding. The affinity assessment was performed with 50% FAD and 50% isopropanol for uncovering any clusters of "hot spots" that FAD would preferentially bind. Due to the limitation of our computing resources, 100% FAD is not feasible. The results revealed 46 hot spots with affinities ranging from 0.2 kcal/mol-3.06 kcal/mol with one area where all FAD hotspots were congregated (Fig. 13A). The transparent sphere with color cold blue to hot red showing the relative "attractiveness" of that spot to FAD. The surface distribution of FAD and isopropanol molecules are depicted in Fig. 13B. The simulation revealed a region with a high affinity to FAD which coincided with the receptor site predicted by Autodock and experimental results by Lippard's group – confirming the easy access of the site (residing to the exterior of the protein) and the feasibility of using FAD as the linker molecule.

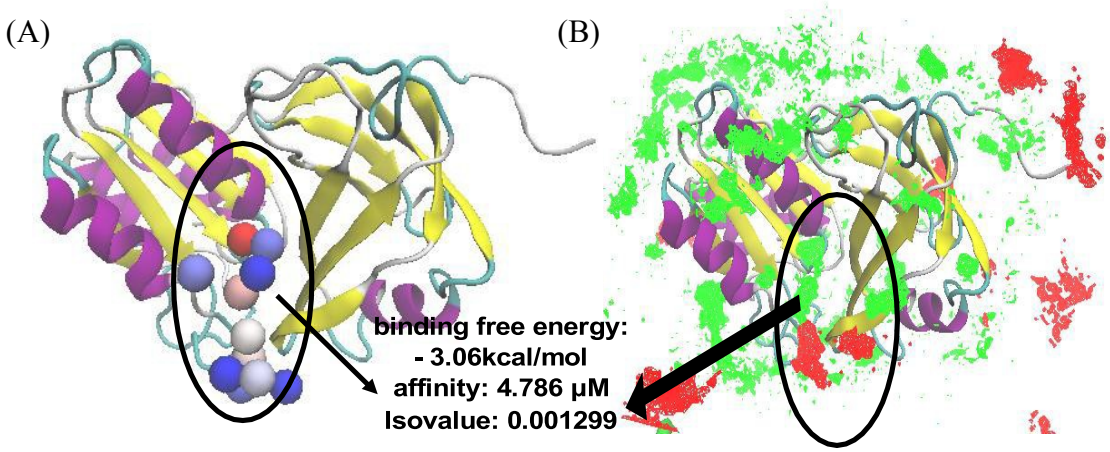

Figure 13: A) The hotspots (blue and red sphere) across the sMMO-Red surface. B) The occupancy grid distribution of the probes (FAD (red), isopropanol (green)) and hotspots (blue and red sphere) across the sMMO-Red surface.

In summary, the analysis suggested that the simulation approach is reliable to be utilized for evaluating binding interactions of modified cofactors. The overall docking and molecular dynamics simulations suggested that based on spatial distribution and binding location, FAD to be the most suitable molecule to be utilized as the linker to attach the enzyme system to an electrode base. In the following sections, how are cofactors modified with linker molecules are discussed. Due to the unavailability of appropriate functional groups, a FAD cannot be directly attached to a metal electrode. However, previous studies with NAD clearly has established the possibility of using Fe-S clusters to attach cofactors to metal surfaces (Mahadevan, Gunawardena et al. 2014, Mahadevan, Gunawardena et al. 2015, Mahadevan, Fernando et al. 2016). In order to perform simulations, FAD functionalized with FeS was used.

3.4.2 Identification of a Ligand Suitable for Anchoring the Enzyme System

(A)

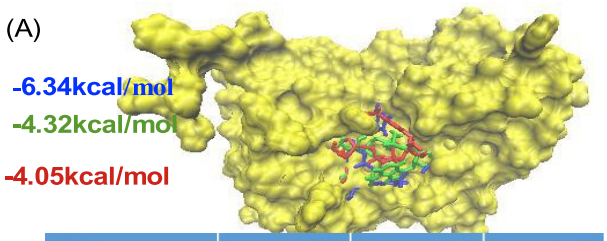

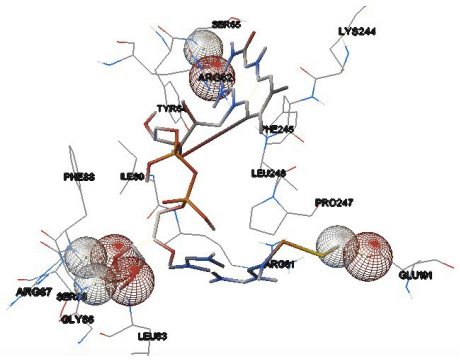

Binding Energy(kcal/mol)	-6.34	-4.32	-4.05
KI(mM)	22.57mM	67mM	100mM
Intermolecular Energy(kcal/mol)	-12.01	-9.99	-9.72
Internal Energy(kcal/mol)	-4.5	-4.32	-3.68

(B)

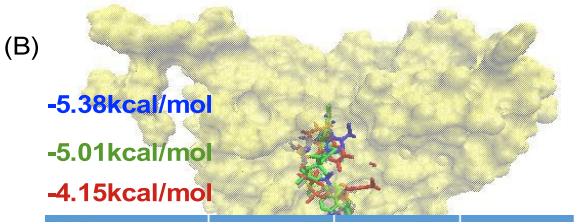

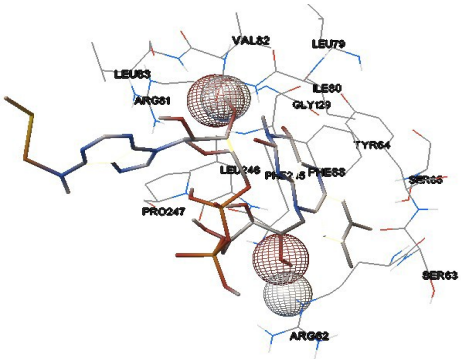

Binding Energy(kcal/mol)	-5.38	-5.01	-4.15
KI(mM)	14.57mM	30.45mM	93.32mM
Intermolecular Energy(kcal/mol)	-12.24	-11.87	-11.01
Internal Energy(kcal/mol)	-7.24	-5.69	-8.54

Figure 14: A) Predicted three most stable conformations of sMMOR (with binding affinity in descending order of blue, green, and red) docked with FAD-FeS, their binding thermodynamics and interactions; B) Conformations of FAD-FeS-Ag.

For FAD to be used as a potential linker molecule to anchor sMMO to a supporting electrode, it critical that the modified coenzyme attaches to the active site unfettered. The most stable binding conformations of a FeS-modified FAD, i.e., FAD-

FeS, FAD-FeS-Ag are depicted in Figure 14. As shown in Figure 14, the top three most possible conformation of FAD-FeS are highly clustered within the same pocket. It is interesting to note that besides the already existed hydrogen bonding between residues Arg62 and Glu191, the newly added [FeS] group created a pair of new bonds at Ser88 and Leu83. It is clear that adding [FeS] further strengthened binding affinity between the FAD and the receptor molecule. Dissociation constant and internal energy are also higher than that of a FAD.

Thermodynamic data clearly rein- forces the argument that FAD-FeS forms a much stronger bond with the receptor as com- pared to FAD alone. Binding conformations of Ag-FeS-modified FAD on sMMOR are depicted in Figure 14B. As can be seen, the top three most stable conformations are highly clustered within the same pocket as before. It could be noted that conformations with FeS were slightly skewed to left or right from the canyon; however, the introduction of Ag corrected the skewing by aligning the molecule along the canyon fitting in better agreement with experimental results (with unmodified NAD). Interestingly, Ag addition removed the extra bonds that appeared leaving existed hydrogen bonding between ligand and Arg62 and otherresidues.

Nevertheless, the binding affinity increase as a result of FeS introduction was impacted only slightly as a result of the further introduction of Ag.

3.4.3 Identification of a Ligand Suitable for Anchoring the Enzyme System

(A)

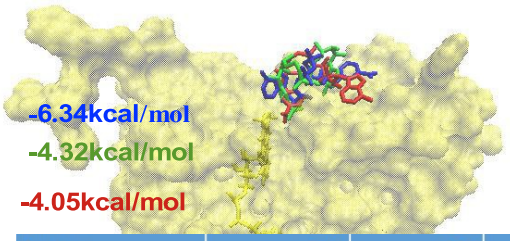

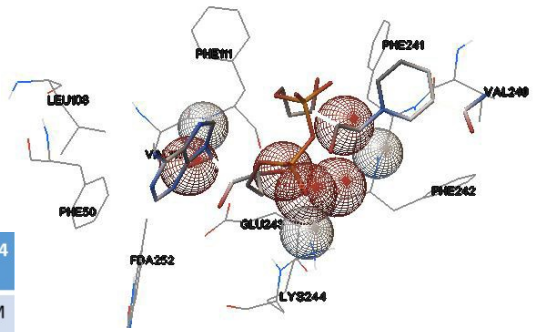

Binding Energy(kcal/mol)	-5.05	-4.93	-4.84
KI(mM)	199.59mM	243.36 mM	285.08mM
Intermolecular Energy(kcal/mol)	-9.52	-9.4	-9.31
Internal Energy(kcal/mol)	-1.97	-0.3	-1.94

B)

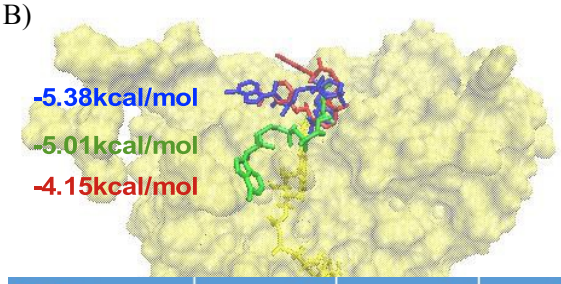

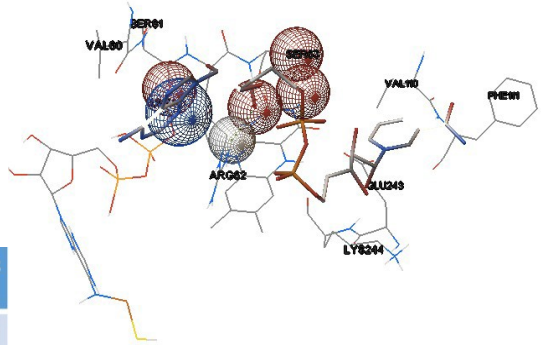

Binding Energy(kcal/mol)	-6.11	-6.0	-5.08
KI(mM)	33.27mM	39.71mM	187.44mM
Intermolecular Energy(kcal/mol)	-10.58	-10.48	-9.56
Internal Energy(kcal/mol)	-0.43	-1.49	-1.41

Figure 15: A) Predicted three most stable conformations of sMMOR (with binding affinity in descending order of blue, green, and red) docked with FAD-FeS, their binding thermodynamics and interactions; B) Conformations of FAD-FeS-Ag.

It should be noted that NAD^+ is an important element in the natural methane oxidation phenomena via sMMOR. Accordingly, it is critical that sulfur-and-metal-modified-FAD introduction still leaves unfettered access of NAD^+ to its natural binding

site. Fig. 15 depicts binding conformations of NAD^+ on sMMO docked with the FAD, and FAD-FeS-Ag. It is clear that NAD^+ docks on to the upper region of the canyon of FAD modified with FeS-Ag as it did with the unmodified FAD. The interaction diagram shows that the hydrogen bonding between residues Val 83, Lys244 and Phe242 formed in the case of NAD^+ interacting with modified FAD and FAD-FeS and FAD-FeS-Ag in the case with the un- modified FAD. Thermodynamic analysis suggests an increase in binding affinities of NAD^+ with modified FAD molecules as it did with modified NAD alone. It is again clear that introduction of Fe-S to the system improves binding affinities of both cofactors likely due to the facilitation of new interactions between residues of the receptor and modified ligands.

3.4.4 Proposed Electron Transport Pathway

A critical requirement for developing an electrode that can electrically communicate with the active site of a redox enzyme is the existence of a path for electrons to flow. Figure 16. A depicts the FAD and NAD^+ conformations with the highest binding affinities in close proximity to each other that allows efficient electron transfer between molecules. A clear pathway for electron transfer in the natural system is postulated along the ridge of the folded protein covering residues 0-45. An electron ejected from NAD will be transferred to FAD and travel through the protein strand to the sMMOH subunit.

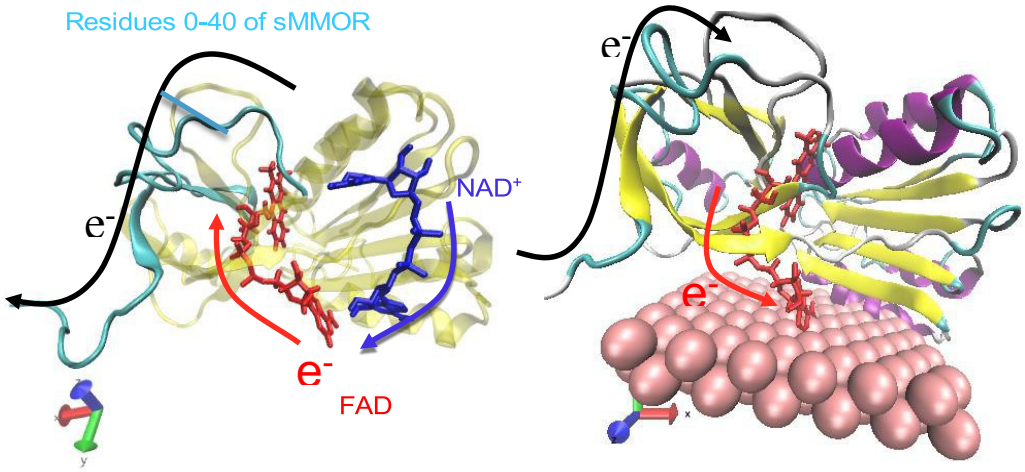

Figure 16: binding conformations of NAD^+ and FAD along with the A) natural and B) proposed electron transport pathways.

Based on above findings, an enzymatic electrode as depicted in Fig. 16 B is proposed where electrons generated by methane oxidation on the sMMOH is routed to the metal electrode via FAD-FeS in the sMMOR subunit. This configuration may allow possible elimination of NAD+ from the system by using a catalyst that would promote oxygen reduction at the cathode (such as Pt (Nørskov, Rossmeisl et al. 2004), lactase (Ghangrekar and Shinde 2007) or cytochrome oxidase (Proietti, Jaouen et al. 2011). Enzymatic fuel cells based on cofactor immobilization have been developed for other enzyme systems including glucose dehydrogenase enzyme (Sato, Togo et al. 2005), lactate dehydrogenase (Park and Zeikus 2003), methanol dehydrogenase (Palmore, Bertschy et al. 1998). However, the feasibility of using cofactors for immobilization of

sMMO has never been demonstrated. The expected half reactions of a methane-oxidizing fuel cell are as follows:

Electrode	**Reaction**	**Reduction potential**
Anode	$CH_4 + 2H_2O = CO_2 + 8H^+ + 8e^-$	-0.25
Cathode	$2O_2 + 8H^+ + 8e^- = 4H_2O$	+0.82
Overall	$CH_4 + 2O_2 = CO_2 + 2H_2O$	-1.07

The fuel cell is expected to generate a theoretical open circuit voltage of -1.07V. If proven via experimentation that NAD^+ could be eliminated, a significant decrease of reduction potential is also expected. This is since electron flow from methane oxidation would have to overcome a significant energy barrier on its way to the cathode if $NADH/NAD^+$, a molecule with a high reduction potential is present. Although the presence of NADH as an electron donor, i.e., a biochemical fuel is common in biological systems, the need to supply NADH as a fuel is not practical in an industrial application such as a fuel cell. However, results from this computational study strongly suggest the possibility of the direct wiring of the methane- oxidizing active site to the supporting electrode via FeS-functionalized FAD eliminating the need of NAD^+ to put together an effective methane-consuming fuel cell.

IV. CONCLUSIONS

Docking studies coupled with molecular dynamics simulations identified FAD to be a feasible linker molecule that could attach sMMOR to a Ag electrode. FAD modification with FeS that was done to facilitate FAD attachment to a metal surface did not interfere with binding interactions. In fact, FeS introduction significantly improved the binding affinity of FAD on sMMOR as compared to unmodified FAD. FeS-modified FAD did not interfere with NAD^+ binding as well; in fact, thermodynamic studies indicated an improvement of NAD^+ binding affinities on sMMOR with the introduction of a FeS-modified FAD. The simulations revealed a clear path of electron transport from NAD+ via FAD and residues 0-40 of sMMOR. The analysis revealed a shorter, thermodynamically more favorable re- turn path if the enzyme system is used as a fuel cell using FeS-modified-FAD as the anchoring molecule. The overall analysis suggests the strong possibility of building a fuel cell that could catalyze methane oxidation using sMMO as the anode biocatalyst.

REFERENCES

Bakan, A., N. Nevins, A. S. Lakdawala and I. Bahar (2013). "Druggability Assessment of Allosteric Proteins by Dynamics Simulations in Presence of Probe Molecules." Biophysical Journal 104(2): 556a.

Baldwin, E., W. A. Baase, X.-j. Zhang, V. Feher and B. W. Matthews (1998). "Generation of ligand binding sites in T4 lysozyme by deficiency-creating substitutions." Journal of molecular biology 277(2): 467-485.

Barik, S. (2004). "When proteome meets genome: the alpha helix and the beta strand of proteins are eschewed by mRNA splice junctions and may define the minimal indivisible modules of protein architecture." Journal of biosciences 29(3): 261-273.

Basch, H., K. Mogi, D. G. Musaev and K. Morokuma (1999). "Mechanism of the Methane → Methanol Conversion Reaction Catalyzed by Methane Monooxygenase: A Density Functional Study." Journal of the American Chemical Society 121(31): 7249-7256.

Best, D. and I. Higgins (1981). "Methane-oxidizing activity and membrane morphology in a methanolgrown obligate methanotroph, Methylosinus trichosporium OB3b." Microbiology 125(1): 73-84.

Chatwood, L. L. (2004). Structural and mutagenesis studies of soluble methane monooxygenase reductase from Methylococcus capsulatus (Bath), Massachusetts Institute of Technology.

Chatwood, L. L., J. Müller, J. D. Gross, G. Wagner and S. J. Lippard (2004). "NMR structure of the flavin domain from soluble methane monooxygenase reductase from Methylococcus capsulatus (Bath)." Biochemistry 43(38): 11983-11991.

Chatwood, L. L., J. Müller, J. D. Gross, G. Wagner and S. J. Lippard (2004). "NMR Structure of the Flavin Domain from Soluble Methane Monooxygenase Reductase from Methylococcus capsulatus (Bath)†." Biochemistry 43(38): 11983-11991.

Colby, J. and H. Dalton (1979). "Characterization of the second prosthetic group of the flavoenzyme NADH–acceptor reductase (component C) of the methane mono-oxygenase from Methylococcus capsulatus (Bath)." Biochemical Journal 177(3): 903-908.

Colby, J., D. I. Stirling and H. Dalton (1977). "The soluble methane mono-oxygenase of Methylococcus capsulatus (Bath). Its ability to oxygenate n-alkanes, n-alkenes, ethers, and alicyclic, aromatic and heterocyclic compounds." Biochemical Journal 165(2): 395-402.

Culpepper, M. A. and A. C. Rosenzweig (2012). "Architecture and active site of particulate methane monooxygenase." Critical reviews in biochemistry and molecular biology 47(6): 483-492.

Dalton, H. (2005). "The Leeuwenhoek Lecture 2000 the natural and unnatural history of methane-oxidizing bacteria." Philosophical Transactions of the Royal Society B: Biological Sciences 360(1458): 1207-1222.

Davies, S. L. and R. Whittenbury (1970). "Fine structure of methane and other hydrocarbon-utilizing bacteria." Microbiology 61(2): 227-232.

De Boer, W. E. and W. Hazeu (1972). "Observations on the fine structure of a methane-oxidizing bacterium." Antonie van Leeuwenhoek 38(1): 33-47.

Deeth, R. J. and H. Dalton (1998). "Methane activation by methane monooxygenase: free radicals, Fe-C bonding, substrate dependent pathways and the role of the regulatory protein." JBIC Journal of Biological Inorganic Chemistry 3(3): 302-306.

Fersht, A. (1999). Structure and mechanism in protein science: a guide to enzyme catalysis and protein folding, Macmillan.

Gassner, G. T. and S. J. Lippard (1999). "Component interactions in the soluble methane monooxygenase system from Methylococcus capsulatus (Bath)." Biochemistry 38(39): 12768-12785.

Ghangrekar, M. and V. Shinde (2007). "Performance of membrane-less microbial fuel cell treating wastewater and effect of electrode distance and area on electricity production." Bioresource Technology 98(15): 2879-2885.

Golabi, S. and H. R. Zare (1999). "Electrocatalytic oxidation of hydrazine at glassy carbon electrode modified with electrodeposited film derived from caffeic acid." Electroanalysis 11(17): 1293-1300.

Goodsell, D. S., G. M. Morris and A. J. Olson (1996). "Automated docking of flexible ligands: applications of AutoDock." Journal of Molecular Recognition 9(1): 1-5.

Gorton, L. and E. Domí (2002). "Electrocatalytic oxidation of NAD (P) H at mediator-modified electrodes." Reviews in Molecular Biotechnology 82(4): 371-392.

Hanson, R. S. and T. E. Hanson (1996). "Methanotrophic bacteria." Microbiological reviews 60(2): 439-471.

Hyder, S., A. Meyers and M. Cayer (1979). "Membrane modulation in a methylotrophic bacterium Methylococcus capsulatus (Texas) as a function of growth substrate." Tissue and Cell 11(4): 597-610.

Jiang, H., Y. Chen, P. Jiang, C. Zhang, T. J. Smith, J. C. Murrell and X.-H. Xing (2010). "Methanotrophs: multifunctional bacteria with promising applications in environmental bioengineering." Biochemical Engineering Journal 49(3): 277-288.

Kao, W.-C., Y.-R. Chen, C. Y. Eugene, H. Lee, Q. Tian, K.-M. Wu, S.-F. Tsai, S. S.-F. Yu, Y.-J. Chen and R. Aebersold (2004). "Quantitative proteomic analysis of metabolic regulation by copper ions in Methylococcus capsulatus (Bath)." Journal of Biological Chemistry 279(49): 51554-51560.

Karyakin, A. A., Y. N. Ivanova and E. E. Karyakina (2003). "Equilibrium (NAD+/NADH) potential on poly (Neutral Red) modified electrode." Electrochemistry communications 5(8): 677-680.

Lee, S. J., M. S. McCormick, S. J. Lippard and U.-S. Cho (2013). "Control of substrate access to the active site in methane monooxygenase." Nature 494(7437): 380-384.

Lin, K.-C. and S.-M. Chen (2006). "Reversible cyclic voltammetry of the NADH/NAD+ redox system on hybrid poly (luminol)/FAD film modified electrodes." Journal of Electroanalytical Chemistry 589(1): 52-59.

Lipscomb, J. D. (1994). "Biochemistry of the soluble methane monooxygenase." Annual Reviews in Microbiology 48(1): 371-399.

Mahadevan, A., T. Fernando and S. Fernando (2016). "Iron–sulfur-based single molecular wires for enhancing charge transport in enzyme-based bioelectronic systems." Biosensors and Bioelectronics 78: 477-482.

Mahadevan, A., D. A. Gunawardena and S. Fernando (2014). Biochemical and Electrochemical Perspectives of the Anode of a Microbial Fuel Cell. Technology and Application of Microbial Fuel Cells, InTech.

Mahadevan, A., D. A. Gunawardena, R. Karthikeyan and S. Fernando (2015). "Potentiometric vs amperometric sensing of glycerol using glycerol dehydrogenase immobilized via layer-by-layer self-assembly." Microchimica Acta 182(3-4): 831-839.

Marafon, E., L. T. Kubota and Y. Gushikem (2009). "FAD-modified SiO2/ZrO2/C ceramic electrode for electrocatalytic reduction of bromate and iodate." Journal of Solid State Electrochemistry 13(3): 377-383.

Merkx, M., D. A. Kopp, M. H. Sazinsky, J. L. Blazyk, J. Müller and S. J. Lippard (2001). "Dioxygen activation and methane hydroxylation by soluble methane monooxygenase: a tale of two irons and three proteins." Angewandte Chemie International Edition 40(15): 2782-2807.

Müller, J., A. A. Lugovskoy, G. Wagner and S. J. Lippard (2002). "NMR Structure of the [2Fe-2S] Ferredoxin Domain from Soluble Methane Monooxygenase Reductase and Interaction with Its Hydroxylase†." Biochemistry 41(1): 42-51.

Murray, E. P., T. Tsai and S. Barnett (1999). "A direct-methane fuel cell with a ceria-based anode." Nature 400(6745): 649-651.

Murrell, J. C., B. Gilbert and I. R. McDonald (2000). "Molecular biology and regulation of methane monooxygenase." Archives of microbiology 173(5): 325-332.

Nordlund, P. (1993). "Crystal structure of a bacterial non-haem iron hydroxylase that catalyses the biological oxidation of methane." Nature 366: 9.

Nørskov, J. K., J. Rossmeisl, A. Logadottir, L. Lindqvist, J. R. Kitchin, T. Bligaard and H. Jonsson (2004). "Origin of the overpotential for oxygen reduction at a fuel-cell cathode." The Journal of Physical Chemistry B 108(46): 17886-17892.

O'Boyle, N. M., M. Banck, C. A. James, C. Morley, T. Vandermeersch and G. R. Hutchison (2011). "Open Babel: An open chemical toolbox." Journal of cheminformatics 3(1): 33.

Österberg, T. and U. Norinder (2001). "Prediction of drug transport processes using simple parameters and PLS statistics The use of ACD/logP and ACD/ChemSketch descriptors." European journal of pharmaceutical sciences 12(3): 327-337.

Palmore, G. T. R., H. Bertschy, S. H. Bergens and G. M. Whitesides (1998). "A methanol/dioxygen biofuel cell that uses NAD+-dependent dehydrogenases as catalysts: application of an electro-enzymatic method to regenerate nicotinamide adenine dinucleotide at low overpotentials." Journal of Electroanalytical Chemistry 443(1): 155-161.

Park, D. H. and J. G. Zeikus (2003). "Improved fuel cell and electrode designs for producing electricity from microbial degradation." Biotechnology and bioengineering 81(3): 348-355.

Proietti, E., F. Jaouen, M. Lefèvre, N. Larouche, J. Tian, J. Herranz and J.-P. Dodelet (2011). "Iron-based cathode catalyst with enhanced power density in polymer electrolyte membrane fuel cells." Nature communications 2: 416.

Sato, F., M. Togo, M. K. Islam, T. Matsue, J. Kosuge, N. Fukasaku, S. Kurosawa and M. Nishizawa (2005). "Enzyme-based glucose fuel cell using Vitamin K 3-immobilized polymer as an electron mediator." Electrochemistry Communications 7(7): 643-647.

Sazinsky, M. H. and S. J. Lippard (2006). "Correlating structure with function in bacterial multicomponent monooxygenases and related diiron proteins." Accounts of chemical research 39(8): 558-566.

Sirajuddin, S., D. Barupala, S. Helling, K. Marcus, T. L. Stemmler and A. C. Rosenzweig (2014). "Effects of zinc on particulate methane monooxygenase activity and structure." Journal of Biological Chemistry 289(31): 21782-21794.

Sirajuddin, S. and A. C. Rosenzweig (2015). "Enzymatic oxidation of methane." Biochemistry 54(14): 2283-2294.

Stainthorpe, A., V. Lees, G. P. Salmond, H. Dalton and J. C. Murrell (1990). "The methane monooxygenase gene cluster of Methylococcus capsulatus (Bath)." Gene 91(1): 27-34.

Walters, K. J., G. T. Gassner, S. J. Lippard and G. Wagner (1999). "Structure of the soluble methane monooxygenase regulatory protein B." Proceedings of the National Academy of Sciences 96(14): 7877-7882.

Wang, W., R. E. Iacob, R. P. Luoh, J. R. Engen and S. J. Lippard (2014). "Electron transfer control in soluble methane monooxygenase." Journal of the American Chemical Society 136(27): 9754-9762.

Whittington, D. A., A. C. Rosenzweig, C. A. Frederick and S. J. Lippard (2001). "Xenon and halogenated alkanes track putative substrate binding cavities in the soluble methane monooxygenase hydroxylase." Biochemistry 40(12): 3476-3482.

Willner, I., V. Heleg-Shabtai, R. Blonder, E. Katz, G. Tao, A. F. Bückmann and A. Heller (1996). "Electrical wiring of glucose oxidase by reconstitution of FAD-modified monolayers assembled onto Au-electrodes." Journal of the American Chemical Society 118(42): 10321-10322.

Yagi, K. and T. Ozawa (1960). "Complex formation of apo-enzyme, coenzyme and substrate of d-amino acid oxidase: I. Kinetic analysis using indicators." Biochimica et biophysica acta 42: 381-387.

Zhang, J. and J. D. Lipscomb (2006). "Role of the C-terminal region of the B component of Methylosinus trichosporium OB3b methane monooxygenase in the regulation of oxygen activation." Biochemistry 45(5): 1459-1469.

Zimmermann, T., M. Soorholtz, M. Bilke and F. Schüth (2016). "Selective Methane Oxidation Catalyzed by Platinum Salts in Oleum at Turnover Frequencies of Large-Scale Industrial Processes." Journal of the American Chemical Society 138(38): 12395-12400.